Sheared turbulence

numerical methods and application to astrophysical disks

Geoffroy Lesur

Institute of Planetology and Astrophysics of Grenoble (France)

Protoplanetary disks

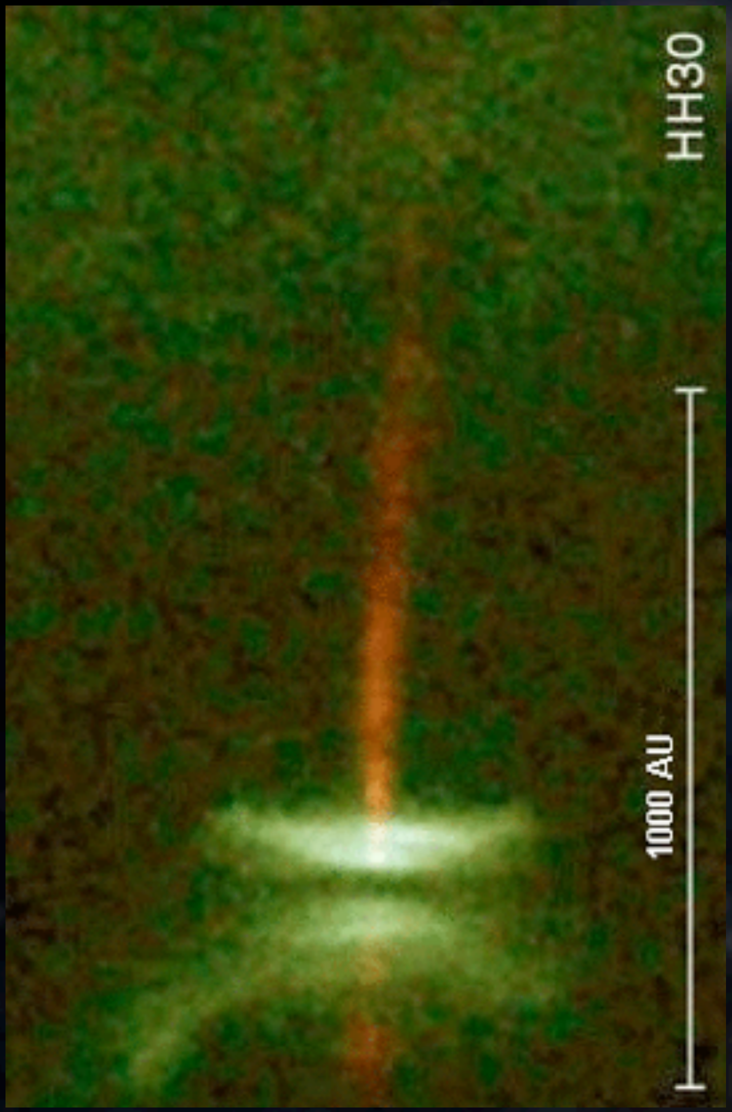

- Size: 10^{11}–10^{15} cm
- Temperature: 10^{3}–10^{1} K
- Number density: 10^{10}—$10^{17}\,\mathrm{cm}^{-3}$
- Ionization fraction: $\sim 10^{-13}$

An accretion problem...

- Accretion discs are known to form around young stars and compact objects
- Gas can fall on the central object only if it looses angular momentum.
- One needs a way to transport angular momentum outward to have accretion:
  «angular momentum transport problem»

First idea: molecular viscosity

- Theoretical accretion rate due to viscous transport is very small compared to observational constrains

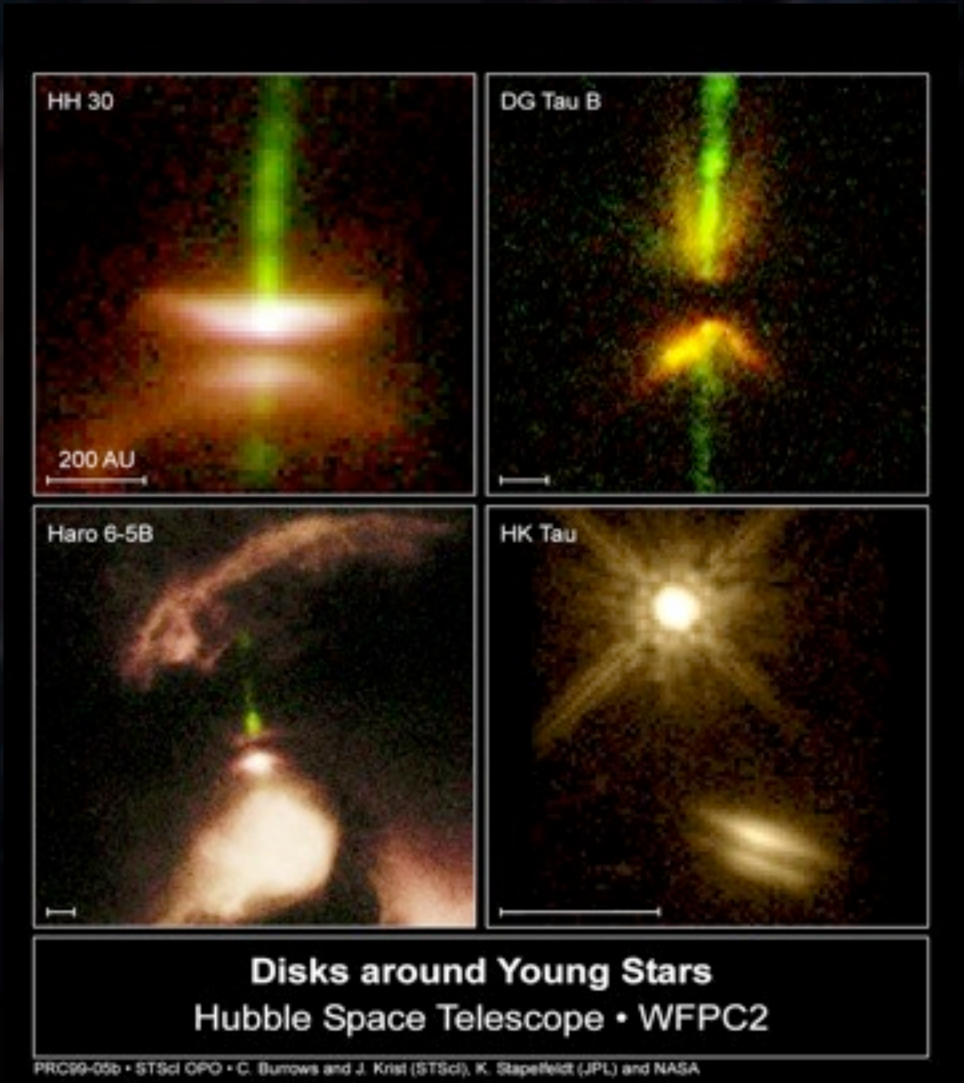

- Other ways to extract angular momentum in discs?

Angular momentum extraction

- Local turbulence
  - Suggested by Shakura & Sunyaev (1973)
  - Turbulence leads to enhanced transport («mixing length theory»).
  - Definition of a turbulent viscosity ν_t

$$10^{-3} < \alpha < 1 \qquad \text{(observations)}$$

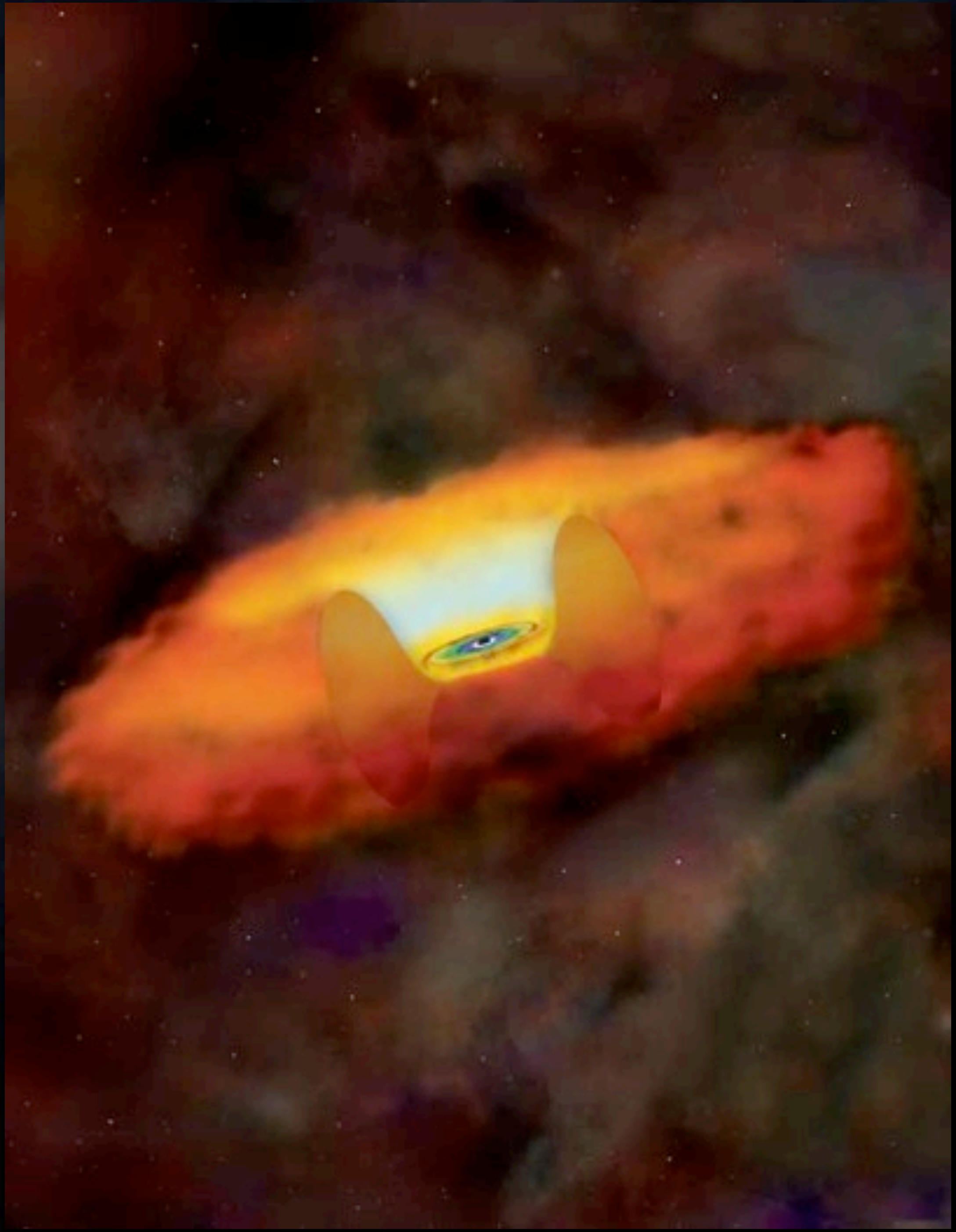

Angular momentum extraction

- Jets
  - Angular momentum extracted by a jet from the disc
  - Most of the gas remains in the disc
  - Many models need turbulence inside the disc to launch jets (e.g. Ferreira & Pelletier 1995)

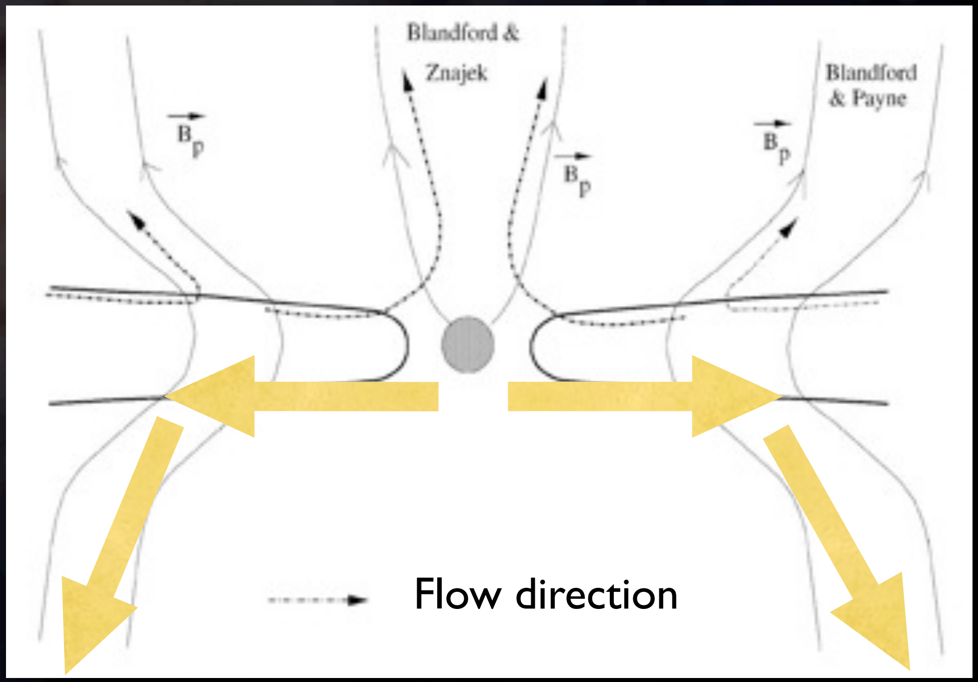

→ Large scale phenomenon which requires large scale magnetic fields

Some disk instabilities

Local instabilities:

- Magnetorotational instability (MRI): shear driven instability but requires an ionised plasma (Velikhov 1959, Chandrasekhar 1960, Balbus & Hawley 1991)
- Subcritical shear instability: probably not efficient enough, if at all (Schartman et al. 2012)
- Baroclinic instabilities: Transport due to waves. Driven by the disk radial entropy profile (Petersen et al. 2007, Lesur & Papaloizou 2010)
- Gravitational instabilities: only for massive & cold enough disk (Gammie 2001)
- Rossby wave instability: requires a local maximum of vortensity (Lovelace et. al 1999)
- Vertical convective instability: Requires a heat source in the midplane (Cabot 1996, Lesur & Ogilvie 2010)

Global instabilities:

- Papaloizou & Pringle instability: density wave reflection on the inner edge (Papaloizou & Pringle 1985)
- Accretion-ejection instability: spiral Alfvén wave reflection on the inner edge (Tagger & Pellat 1999)

The shearing box model

Problem:

- Computing a full disk is computationally expensive

→ Local resolution is poor

→ Boundary conditions

Goal:

- Define a simplified setup which mimics the local properties of an accretion disks

→ Simplifies numerical simulations & boundary conditions

→ Better convergence properties

The incompressible shearing box model

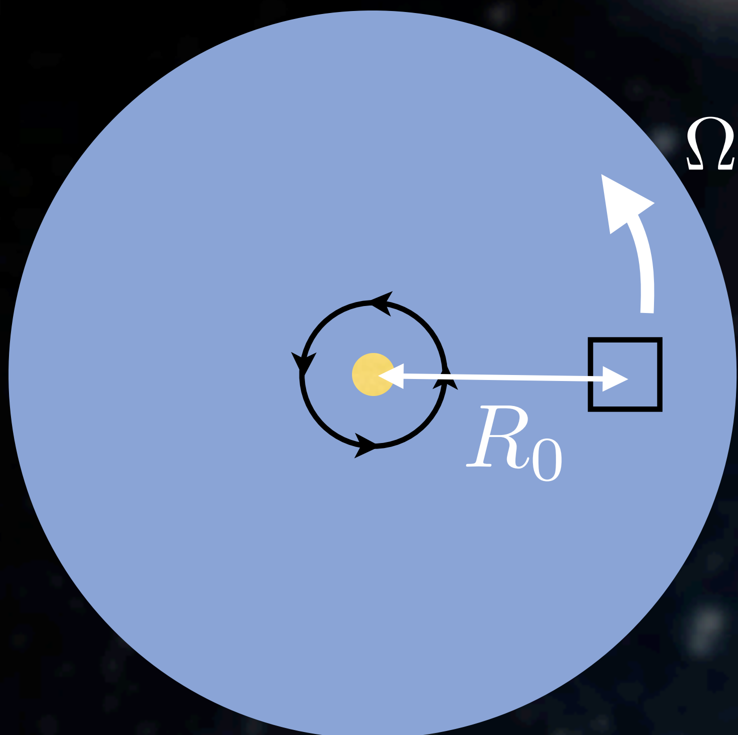

$\Omega(R_0) \equiv \Omega_0$

$$
\begin{aligned}
\nabla \cdot \boldsymbol{u} &= 0 \\
\partial_t \boldsymbol{u} + \boldsymbol{u} \cdot \nabla \boldsymbol{u} &= -\nabla P + \boldsymbol{B} \cdot \nabla \boldsymbol{B} \\
&\quad -2\boldsymbol{\Omega_0} \times \boldsymbol{u} - \nabla \psi + \nu \Delta \boldsymbol{u} \\
\partial_t \boldsymbol{B} &= \nabla \times (\boldsymbol{u} \times \boldsymbol{B}) + \eta \Delta \boldsymbol{B}
\end{aligned}
$$

With the effective potential: $\psi = -q\Omega_0^2 x^2$

Assuming $\Omega(R) \sim R^{-q}$

This set of equations admits a simple solution (incompressible approximation):

$\boldsymbol{u} = -q\Omega_0 x \boldsymbol{e_y}$ → Mean keplerian shear

The incompressible shearing box model

Separate the mean shear from the fluctuations:

$$\boldsymbol{u} = -q\Omega x \boldsymbol{e_y} + \boldsymbol{v}$$

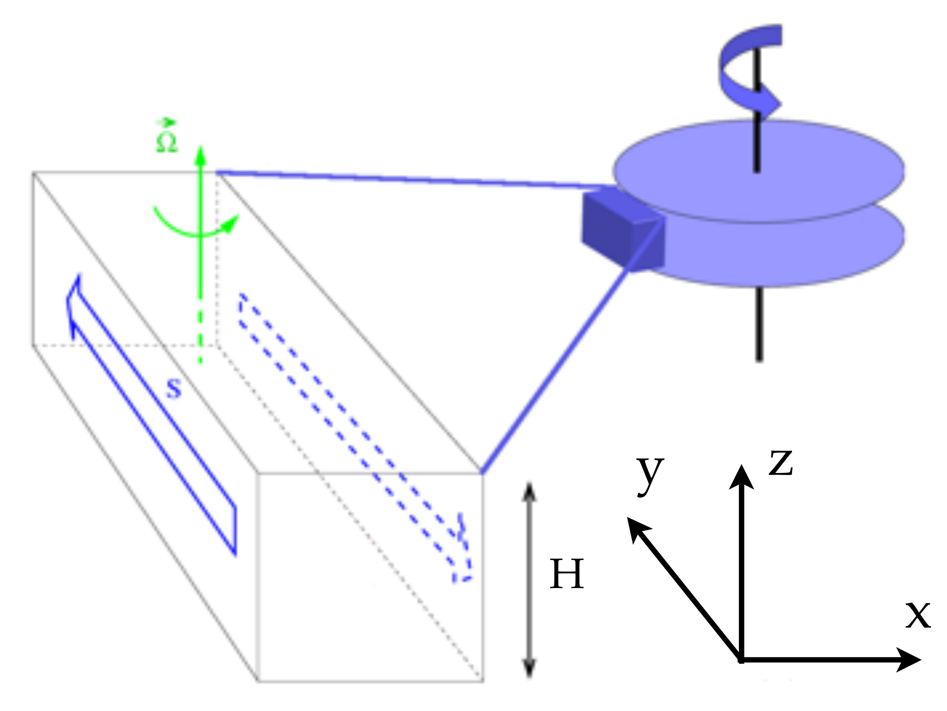

Shearing box equations:

$$\begin{aligned}
\boldsymbol{\nabla} \cdot \boldsymbol{v} &= 0 \\
\partial_t \boldsymbol{v} - q\Omega x \partial_y \boldsymbol{v} + \boldsymbol{v} \cdot \boldsymbol{\nabla} \boldsymbol{v} &= -\boldsymbol{\nabla} P + \boldsymbol{B} \cdot \boldsymbol{\nabla} \boldsymbol{B} - 2\boldsymbol{\Omega} \times \boldsymbol{v} \\
&\quad + q\Omega v_x \boldsymbol{e_y} + \nu \Delta \boldsymbol{v} \\
\partial_t \boldsymbol{B} - q\Omega x \partial_y \boldsymbol{B} &= \boldsymbol{\nabla} \times (\boldsymbol{v} \times \boldsymbol{B}) - q\Omega B_x \boldsymbol{e_y} + \eta \Delta \boldsymbol{B}
\end{aligned}$$

Boundary conditions

Boundary conditions

- Use shear-periodic boundary conditions= «shearing-sheet»
- Allows one to use a sheared Fourier Basis
- periodic in *y* and z (non stratified box)

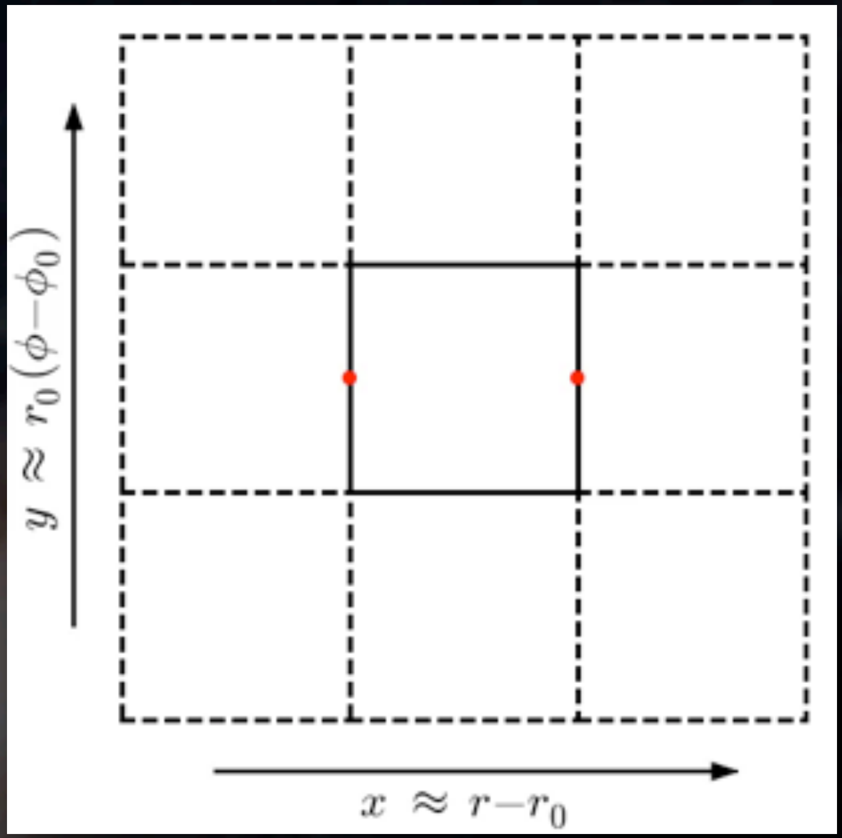

Courtesy T. Heinemann

Vertical and toroidal total magnetic flux conserved

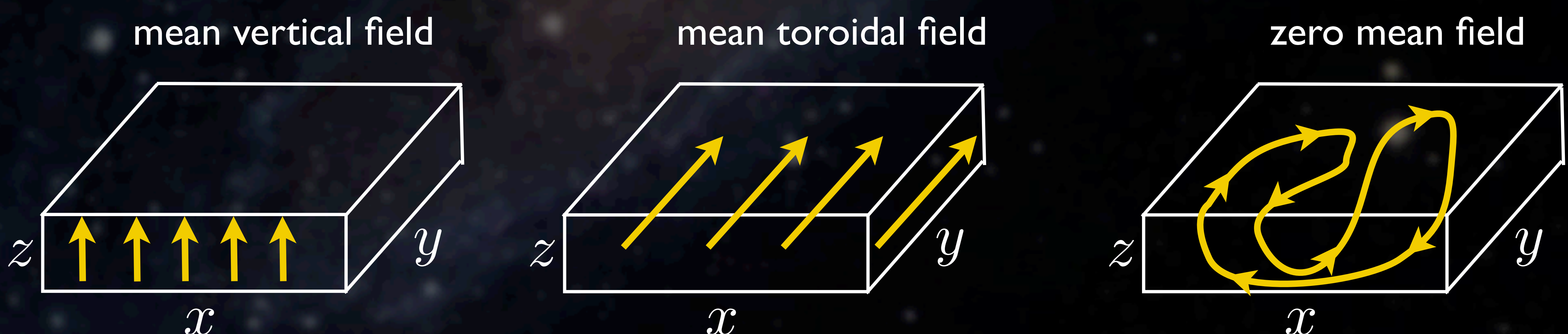

Spectral methods for shearing boxes

Shearing wave

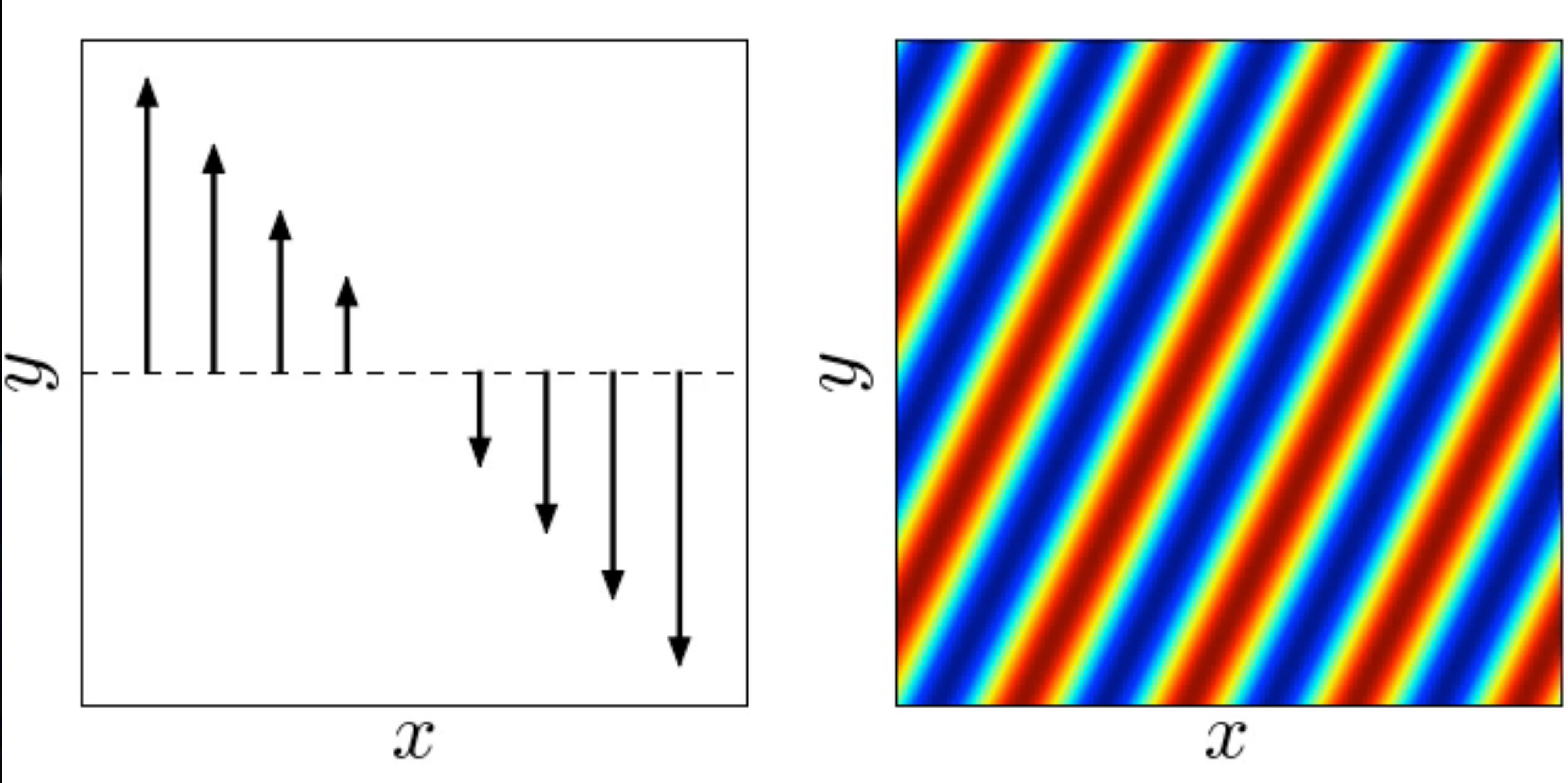

Courtesy T. Heinemann

Spectral methods for shearing boxes

The shearing box involves equations of the type:

$$\frac{\partial Q}{\partial t} - q\Omega x \frac{\partial Q}{\partial y} = H(Q)$$

Assume Q can be decomposed into:

$$Q(t,\boldsymbol{x}) = \tilde{Q}(t)\exp\left[i\boldsymbol{k}(t)\cdot\boldsymbol{x}\right]$$

One has:

$$\frac{\partial Q}{\partial t} = \left[\frac{d\tilde{Q}}{dt} + i\tilde{Q}\frac{d\boldsymbol{k}}{dt}\cdot\boldsymbol{x}\right]\exp\left[i\boldsymbol{k}(t)\cdot\boldsymbol{x}\right]$$

$$\longrightarrow \quad \frac{d\tilde{Q}}{dt} + i\tilde{Q}\frac{d\boldsymbol{k}}{dt}\cdot\boldsymbol{x} - iq\Omega x k_y = \widetilde{H(Q)}$$

Cancel explicit *x* dependency:

$$\frac{dk_x}{dt} = q\Omega k_y \quad \longrightarrow \quad \begin{aligned} &\boldsymbol{k} = \boldsymbol{k}_0 + q\Omega t k_y \boldsymbol{e_x} \\ &\frac{d\tilde{Q}}{dt} = \widetilde{H(Q)} \end{aligned}$$

The Snoopy code
a spectral method for sheared flows

- MHD equations solved in the sheared frame
- Compute non linear terms using a pseudo spectral representation
- 3rd order low storage Runge-Kutta integrator
- Non-ideal effects: Ohmic, Hall, ambipolar (coming soon), Braginskii
- Available online http://ipag.osug.fr/~glesur/snoopy.html

Advantages:

  - Shearing waves are computed exactly (natural basis)
  - Exponential convergence
  - Magnetic flux conserved to machine precision
  - Sheared frame & incompressible approximation: no CFL constrain due to the background sheared flow/sound speed.

Magnetorotational instability

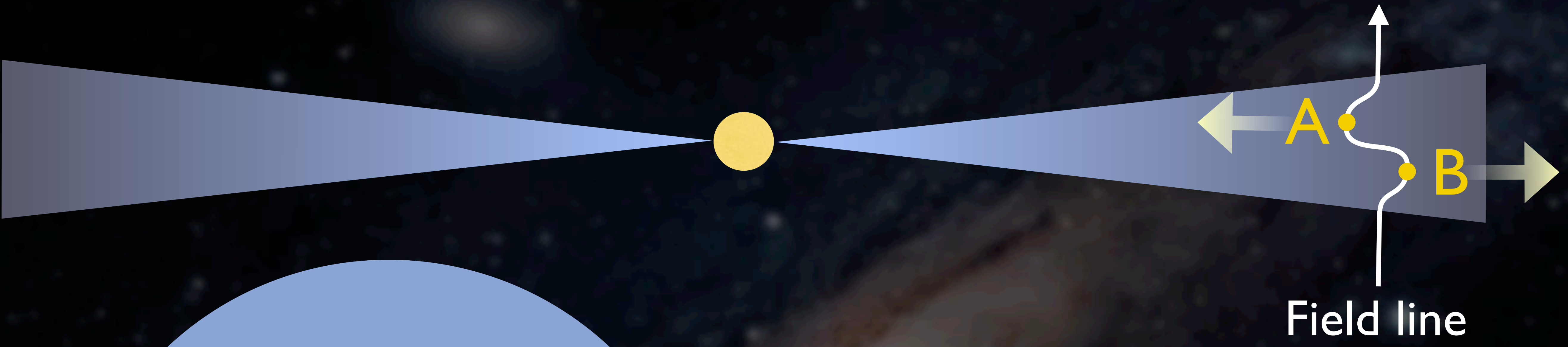

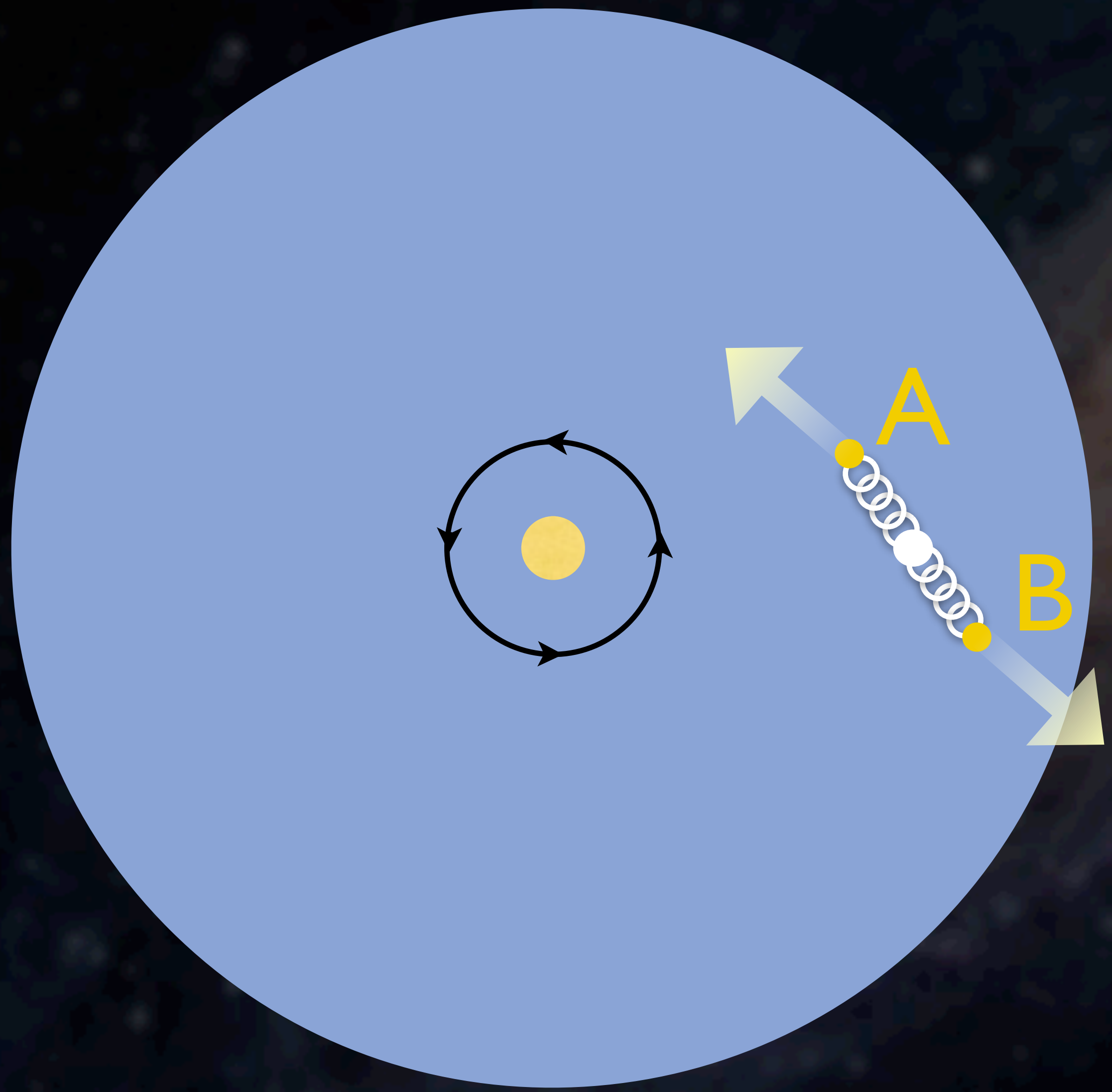

Main properties

- Due to an interaction between magnetic tension and epicyclic motions
- Not too strong magnetic fields required («weak field instability»)
- Need a sufficiently high ionization fraction

Balbus & Hawley 1991, Balbus 2003

MRI simulations

Typical simulation

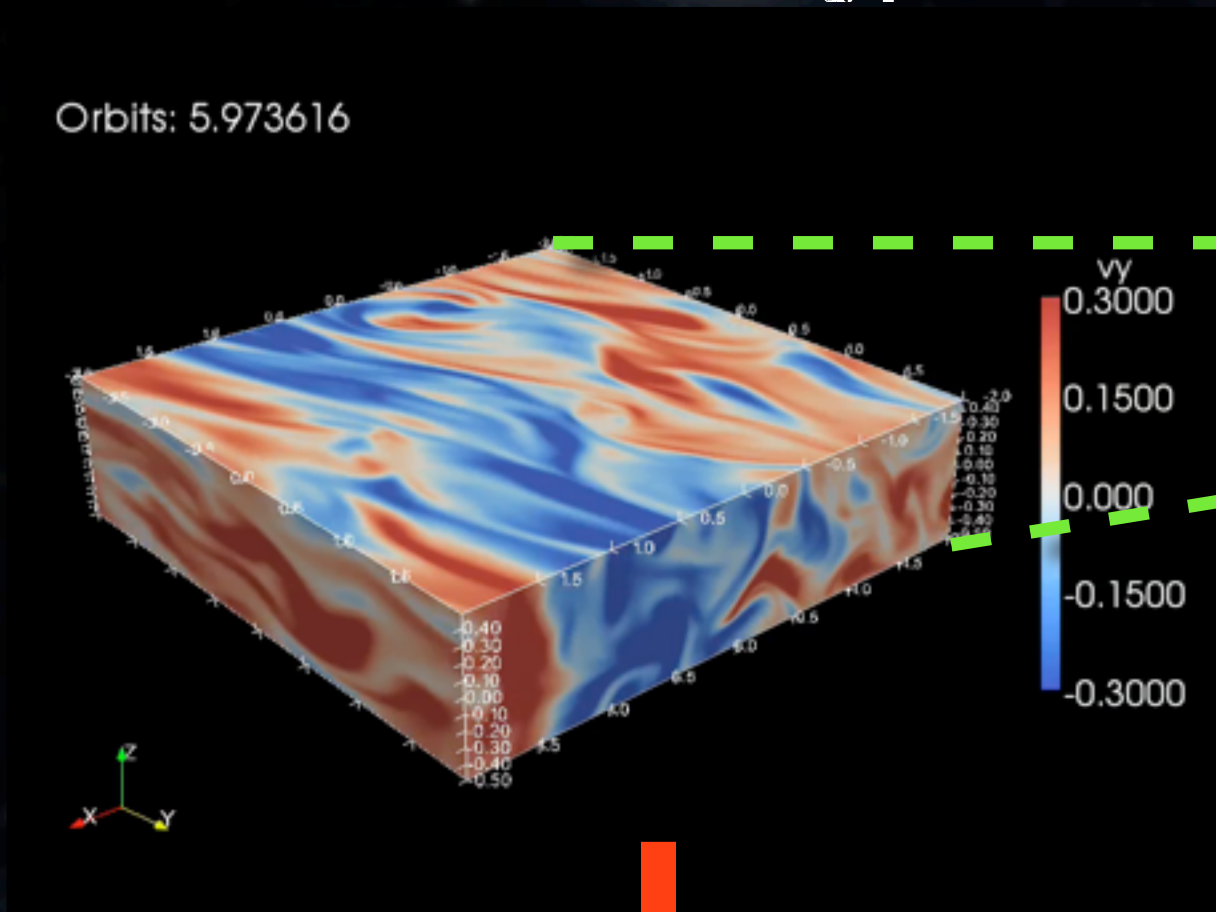

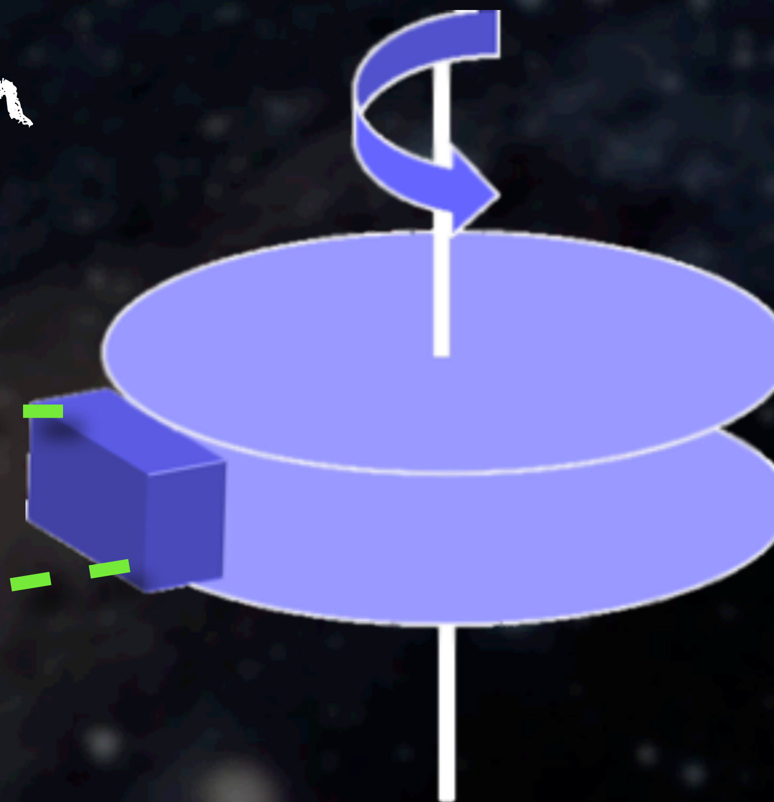

Simulation parameters: Re=1000, Pm=1, β=1000
3D map of vy (azimuthal velocity)

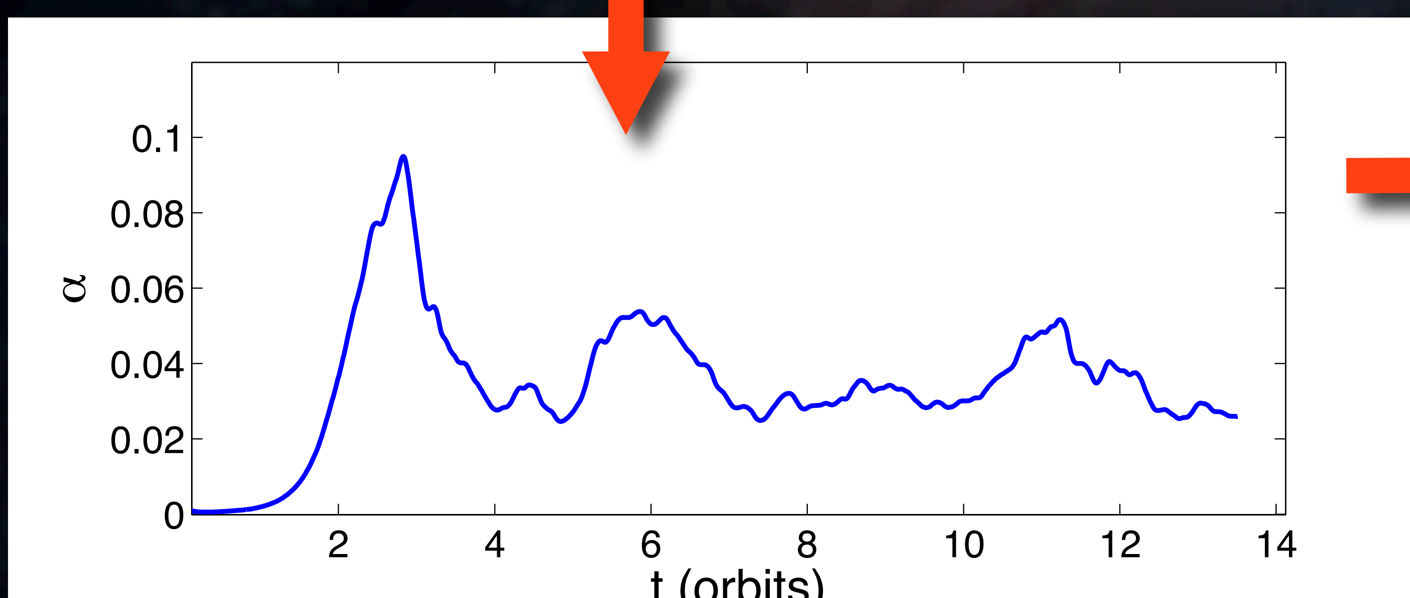

It works!

Is it the end of the story?

Magnetic Prandtl numbers in astrophysics

- Prandtl number (Pm) compares the Ohmic diffusion time to the viscous diffusion time.
- In astrophysical objects, $Pm \ll 1$ or $Pm \gg 1$ ...

$Pm \sim 10^{-6}$

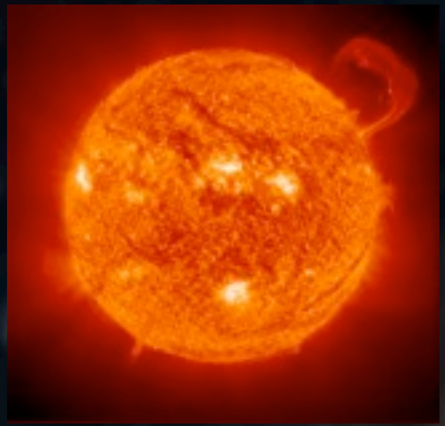

$Pm \sim 10^{-5}$—10^{-2}

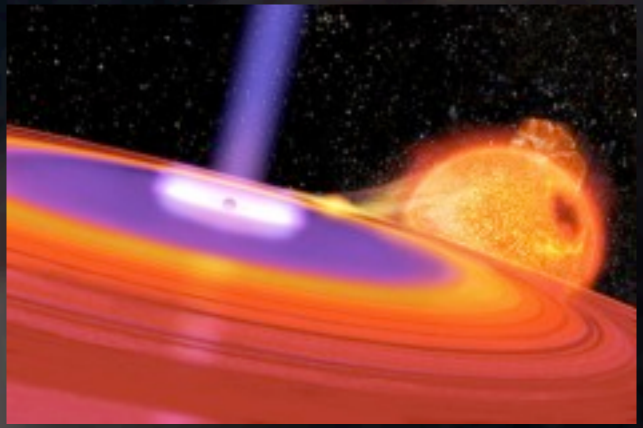

$Pm \sim 10^{-5}$—10^{4}

$Pm \gg 1$

- Problem:

$0.1 < Pm < 100$

MRI simulations

Simulations with a mean vertical field

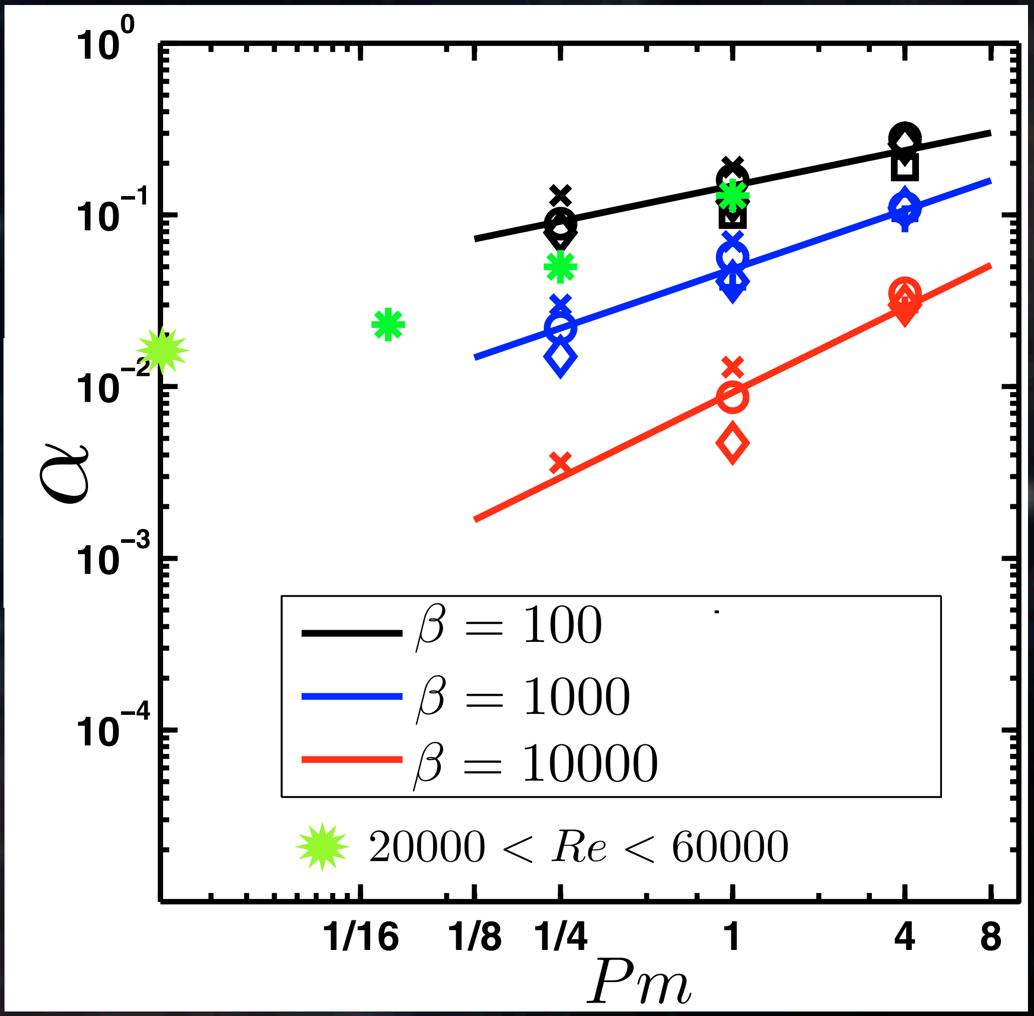

Longaretti & Lesur (2010)

Turbulent transport varies by 2 order of magnitude!

$$\alpha = \alpha(Pm, \beta)$$

MRI simulations

Simulations with a mean toroidal field

Simon & Hawley (2009)

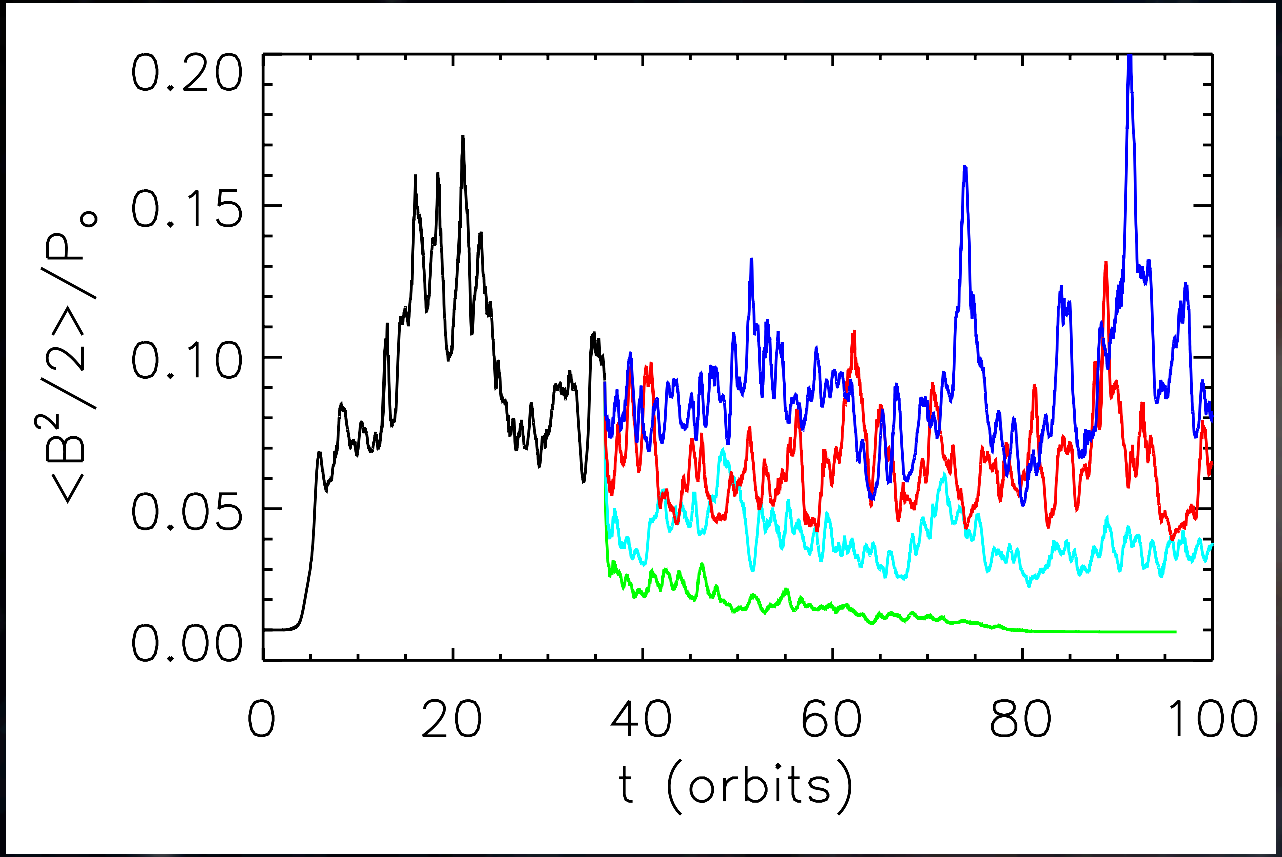

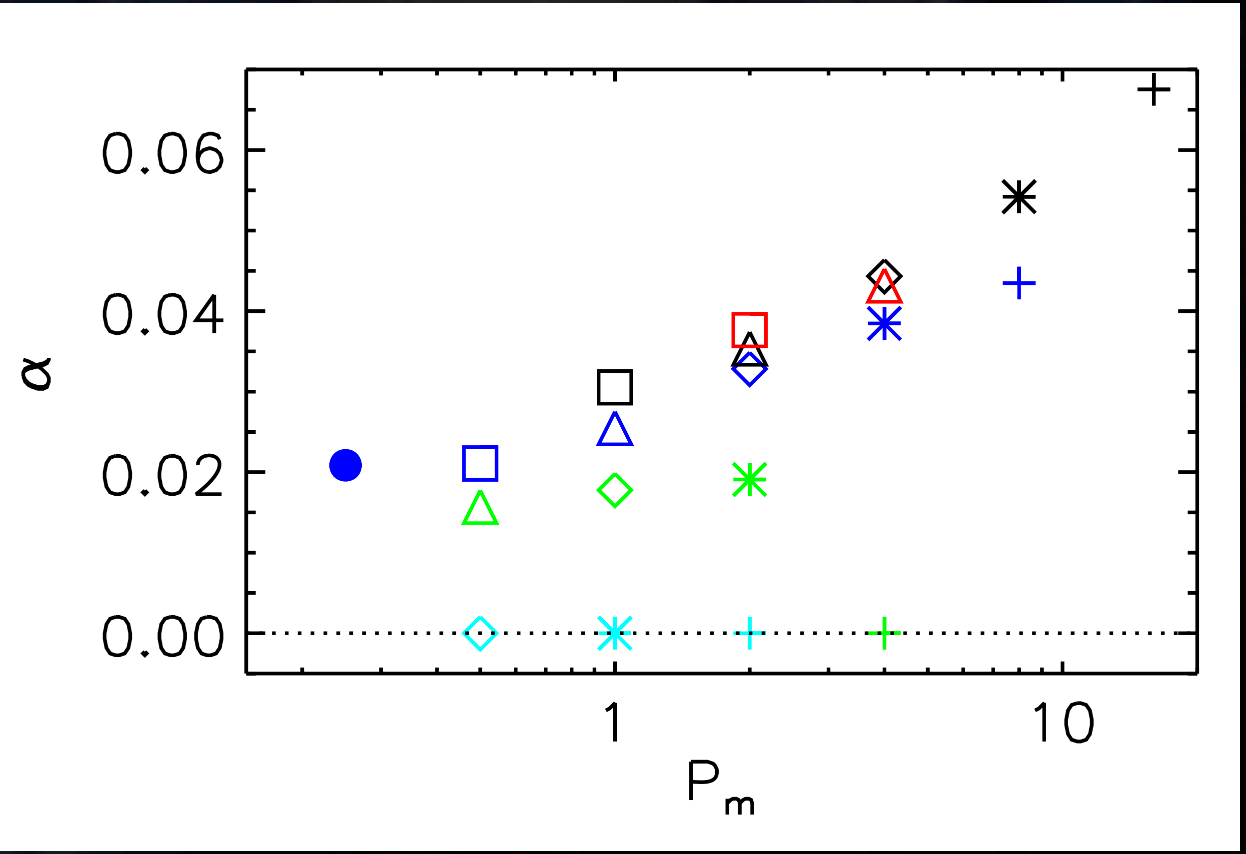

$\beta = 100$

- Weaker transport with a mean toroidal field
- Same trend with *Pm*

$$\rightarrow \alpha = \alpha(Pm, \beta, \mathrm{topology})$$

MRI simulations

Simulations with no mean field
aka «MRI dynamo»

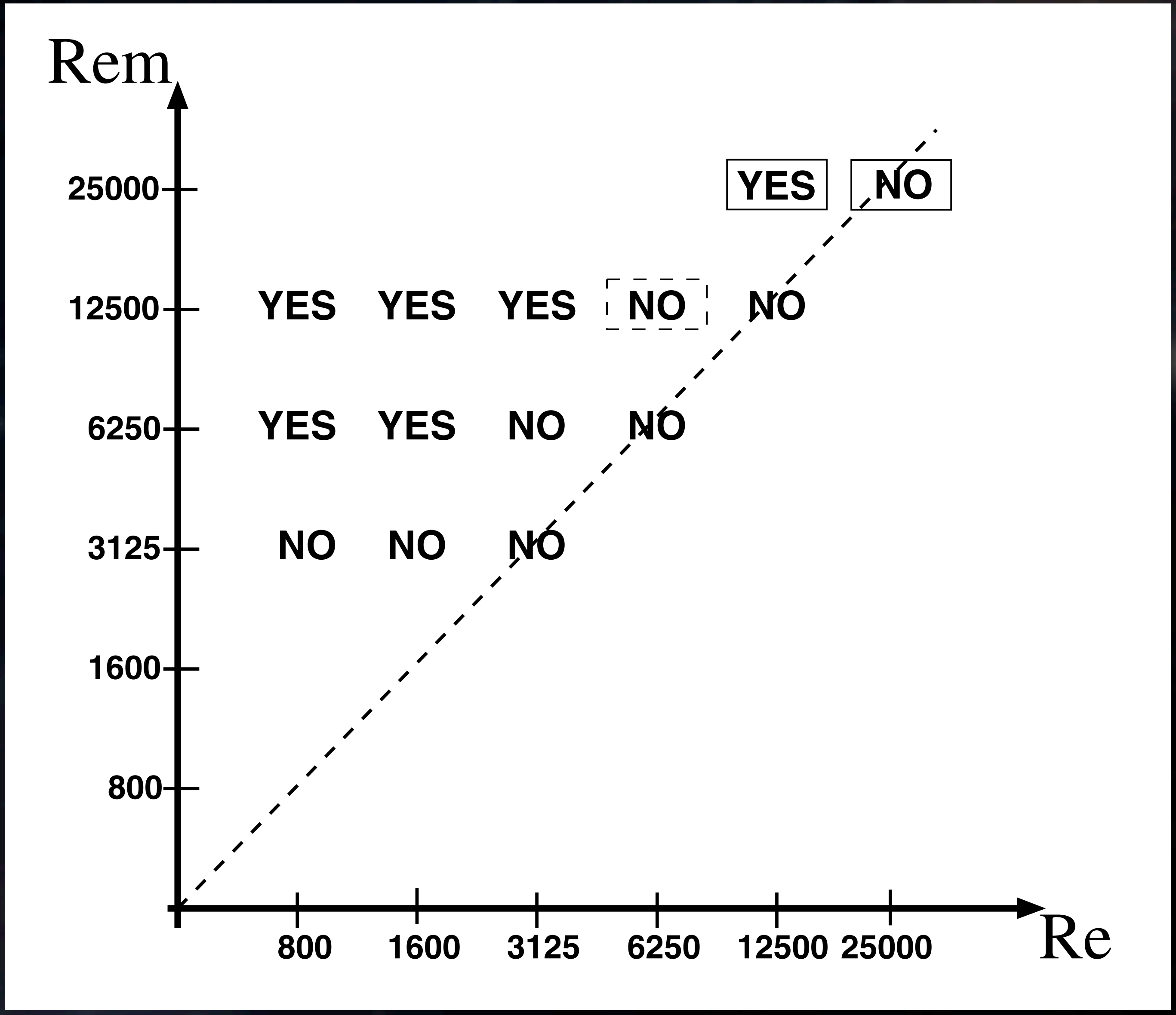

Fromang *et al.* 2007

See also F. Rincon's talk

MRI simulations

Simulations with a mean field

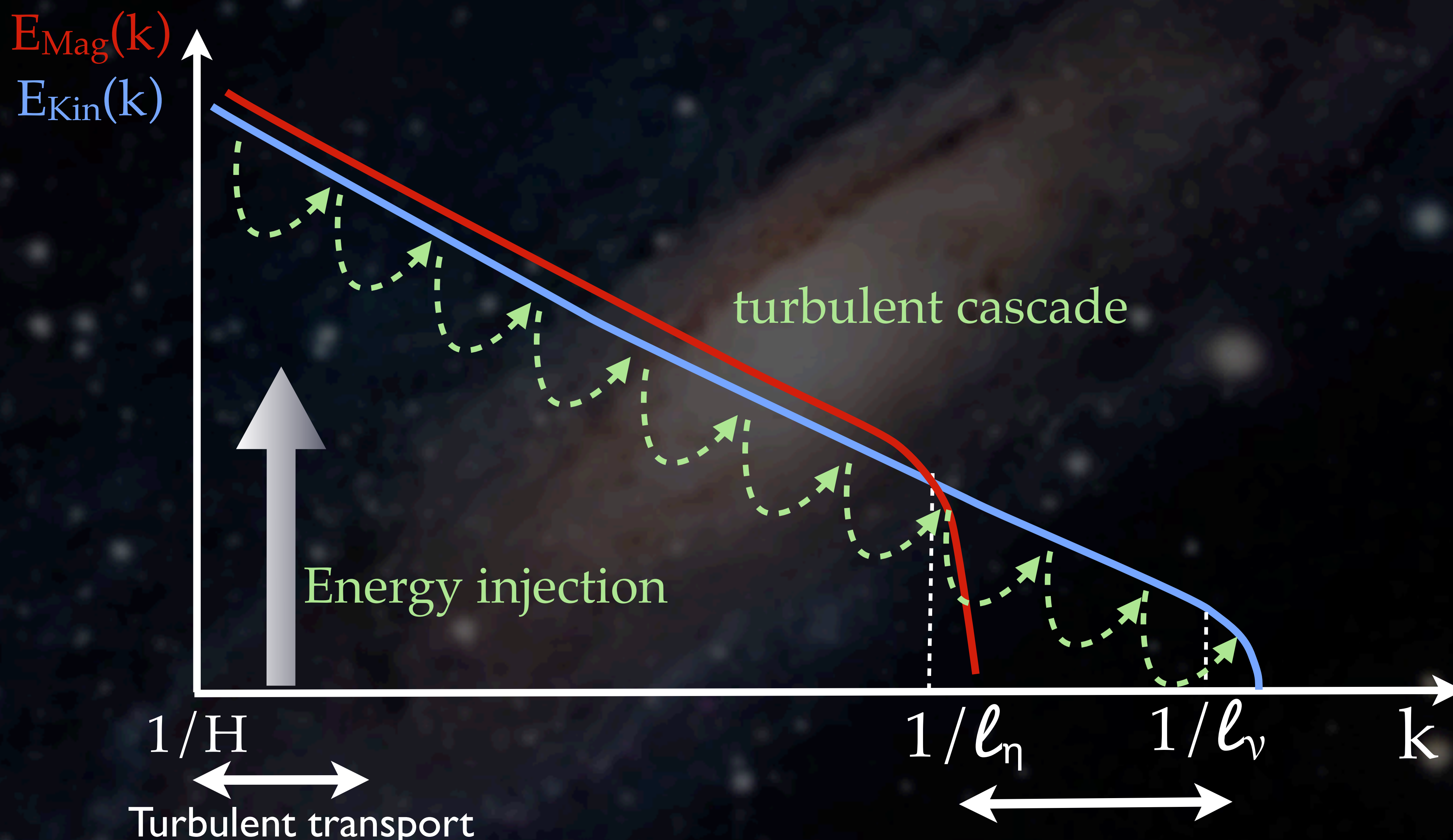

MRI simulations
Typical spectrum

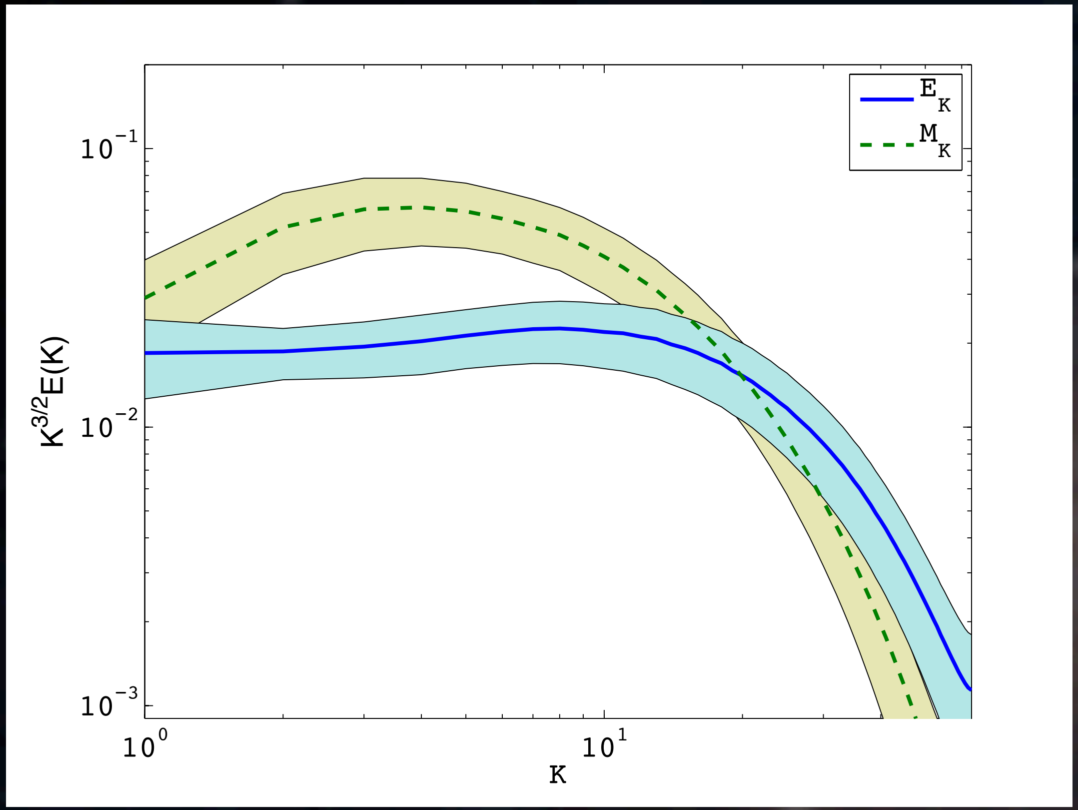

Mean z field, Pm=1/4

Lesur & Longaretti 2011

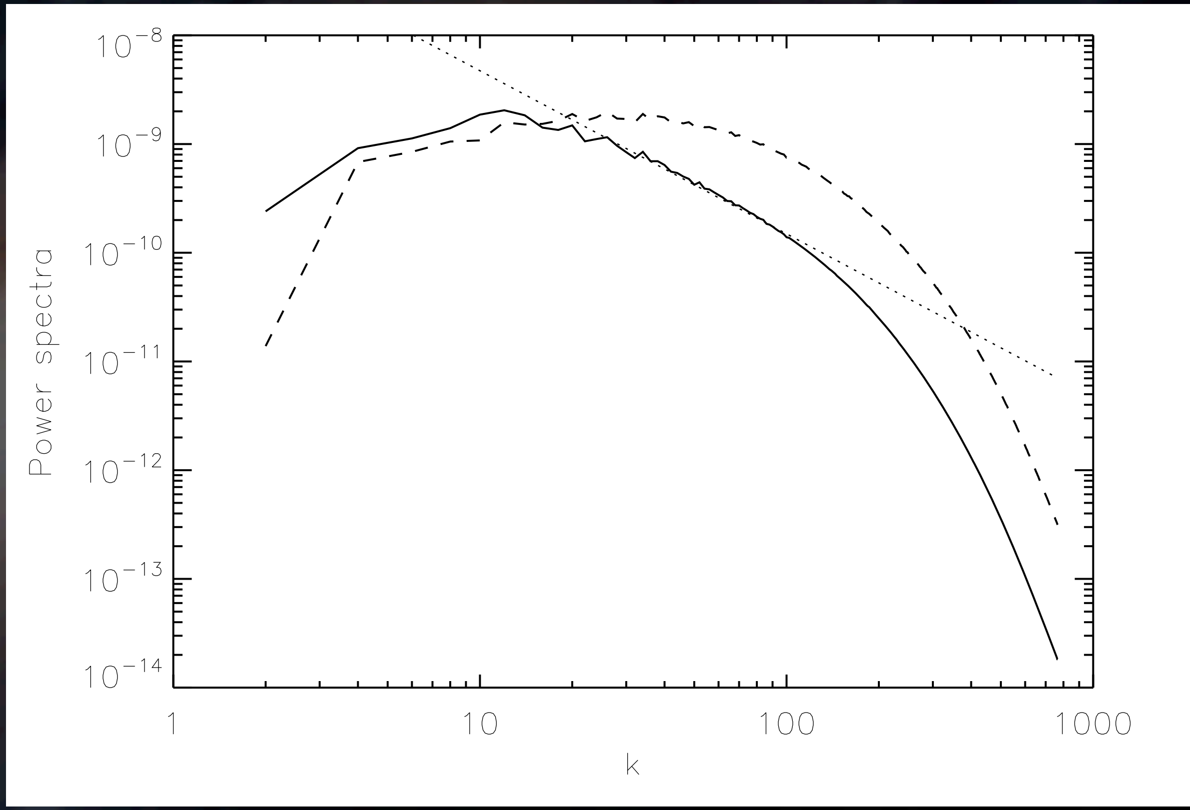

No mean field, Pm=4

Fromang 2010

$K^{-3/2}$ for kinetic energy?

Energy injection

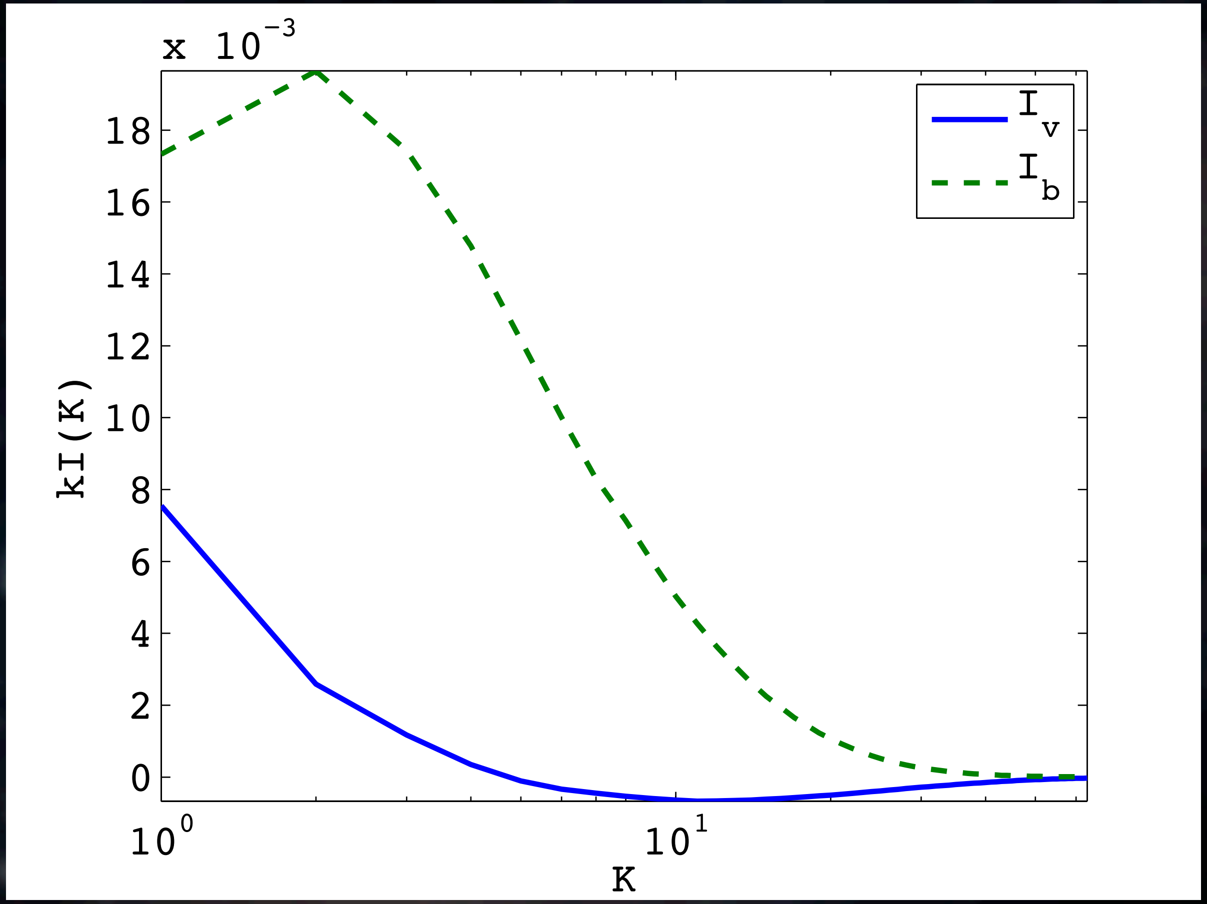

Mean z field, Pm=1/4

- Injection scale not well defined
- MRI is active on a broad range of scales

Anisotropy

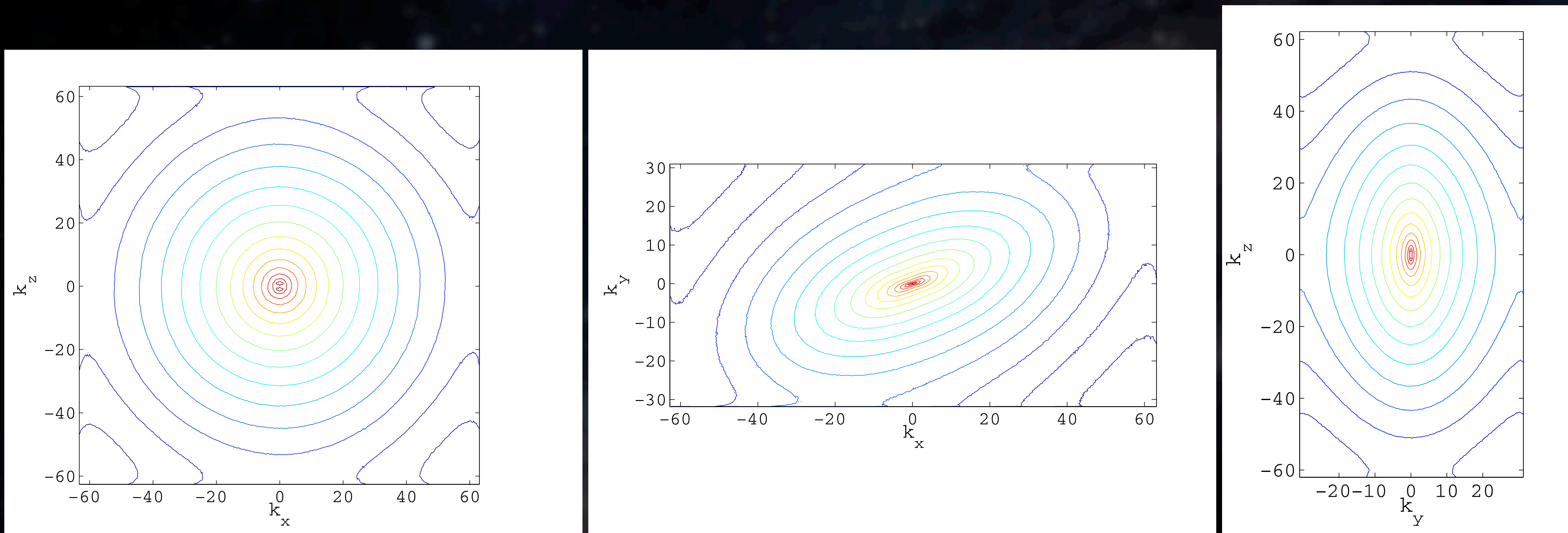

Mean z field, Pm=1/4

- No anisotropy associated to the guide field $\left(\frac{\delta B}{B_Z^0} \gg 1\right)$
- Strong *x-y* anisotropy due to the shear

Magnetic & Cross helicity

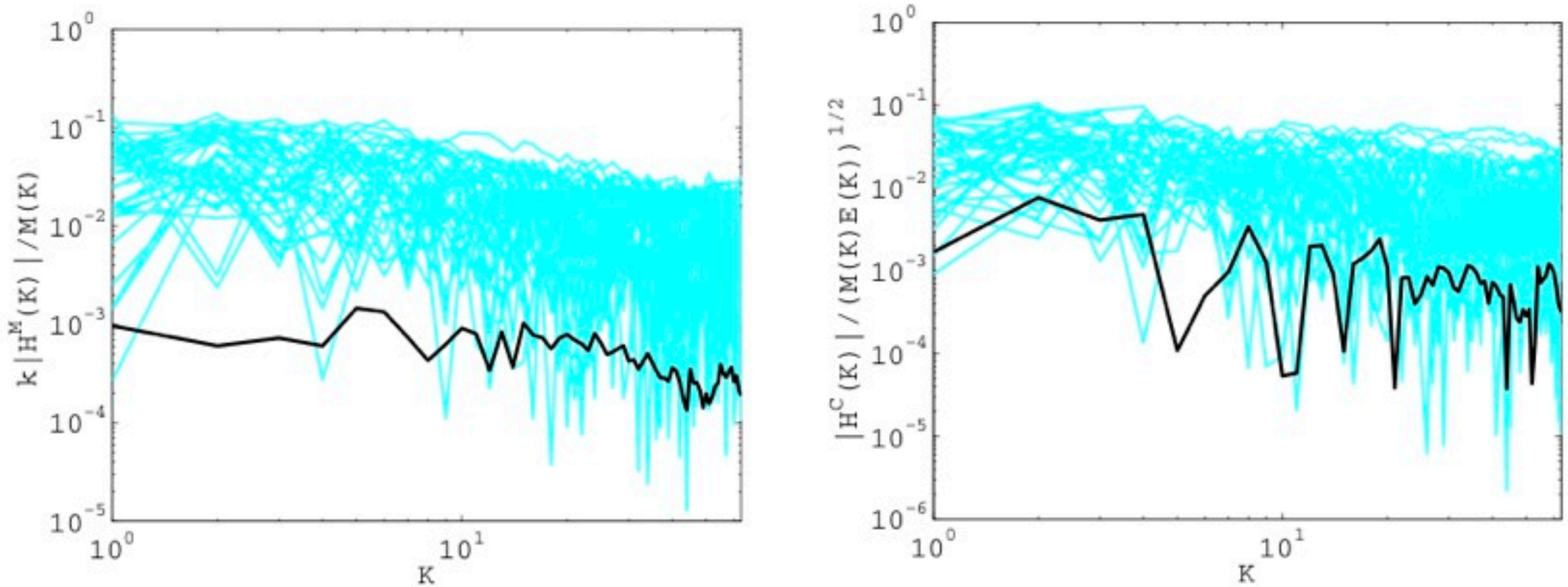

Fig. 4. Average relative magnetic helicity (*left*) and cross helicity (*right*) spectra in the $Pm = 0.25$ case (black lines). Instantaneous spectra are represented in light blue. The absolute value of relative helicities is plotted here, since the helicity sign is constantly changing.

Magnetic helicity cascade arguments seem to be irrelevant

MRI simulations

Simulations with a mean field

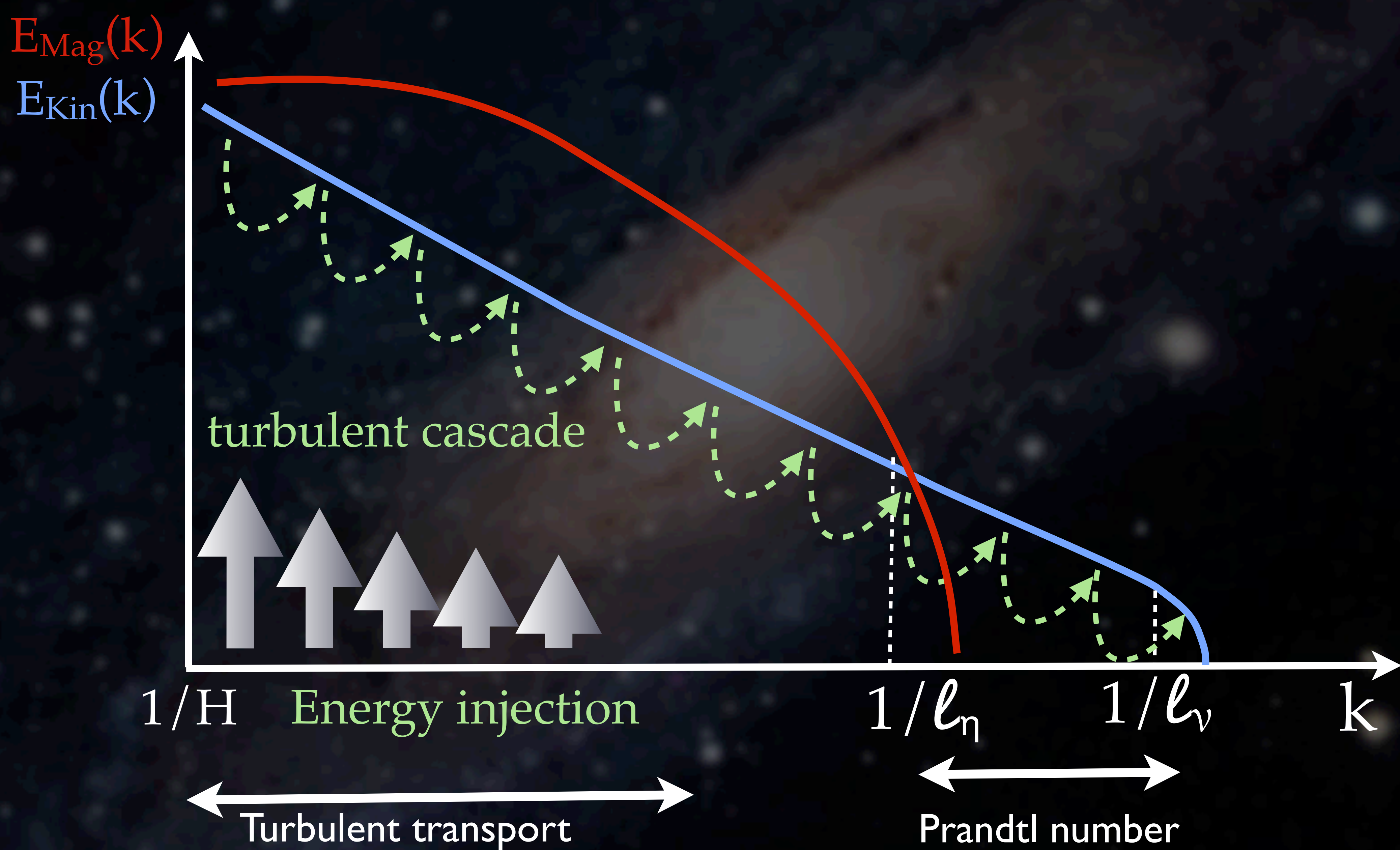

Probing the turbulent cascade

Energy transfers are due to nonlinear terms

$$\partial_t \boldsymbol{v} = -\boldsymbol{v}\cdot\boldsymbol{\nabla}\boldsymbol{v} + \boldsymbol{B}\cdot\boldsymbol{\nabla}\boldsymbol{B} + \dots$$
$$\partial_t \boldsymbol{B} = -\boldsymbol{v}\cdot\boldsymbol{\nabla}\boldsymbol{B} + \boldsymbol{B}\cdot\boldsymbol{\nabla}\boldsymbol{v} + \dots$$

Consider the energy budget for a given Fourier mode

$$\partial_t \frac{|\hat{\boldsymbol{v}}_k|^2}{2} = -\sum_{q+p=k} i(\hat{\boldsymbol{v}}_k^*\cdot\hat{\boldsymbol{v}}_q)(\hat{\boldsymbol{v}}_p\cdot\boldsymbol{k}) + \sum_{q+p=k} i(\hat{\boldsymbol{v}}_k^*\cdot\hat{\boldsymbol{b}}_q)(\hat{\boldsymbol{b}}_p\cdot\boldsymbol{k}) + \dots$$

$$\partial_t \frac{|\hat{\boldsymbol{B}}_k|^2}{2} = -\sum_{q+p=k} i(\hat{\boldsymbol{b}}_k^*\cdot\hat{\boldsymbol{b}}_q)(\hat{\boldsymbol{v}}_p\cdot\boldsymbol{k}) + \sum_{q+p=k} i(\hat{\boldsymbol{b}}_k^*\cdot\hat{\boldsymbol{v}}_q)(\hat{\boldsymbol{b}}_p\cdot\boldsymbol{k}) + \dots$$

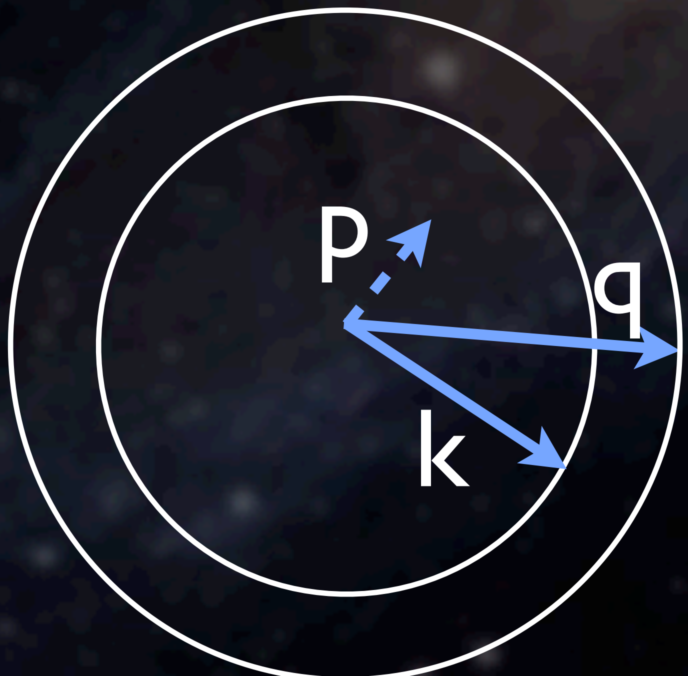

In the triad interaction, energy is transferred from k to q.
p is an intermediate.

Probing the turbulent cascade

Introduce shell filtered fields

$$\boldsymbol{v}_K(\boldsymbol{x}) = \sum_{K<|\boldsymbol{k}|\leq K+1} \widehat{\boldsymbol{v}}(\boldsymbol{k})\exp(i\boldsymbol{k}\cdot\boldsymbol{x}) \qquad \boldsymbol{B}_K(\boldsymbol{x}) = \sum_{K<|\boldsymbol{k}|\leq K+1} \widehat{\boldsymbol{B}}(\boldsymbol{k})\exp(i\boldsymbol{k}\cdot\boldsymbol{x})$$

One defines spectral transfer functions as Alexakis et al. (2007):

$$\begin{aligned}
T_{vv}(Q,K) &= -\int \boldsymbol{v}_K\cdot(\boldsymbol{v}\cdot\boldsymbol{\nabla}\boldsymbol{v}_Q)\,d\boldsymbol{x}^3 \\
T_{bb}(Q,K) &= -\int \boldsymbol{B}_K\cdot(\boldsymbol{v}\cdot\boldsymbol{\nabla}\boldsymbol{B}_Q)\,d\boldsymbol{x}^3 \\
T_{bv}(Q,K) &= \int \boldsymbol{v}_K\cdot(\boldsymbol{B}\cdot\boldsymbol{\nabla}\boldsymbol{B}_Q)\,d\boldsymbol{x}^3 \\
T_{vb}(Q,K) &= \int \boldsymbol{B}_K\cdot(\boldsymbol{B}\cdot\boldsymbol{\nabla}\boldsymbol{v}_Q)\,d\boldsymbol{x}^3
\end{aligned}$$

- *$T_{ij}(Q,K)$:* Transfer rate of energy (kinetic or magnetic) from shell Q to shell K
- *CAUTION:* Transfer functions should be computed with the *same numerical algorithm* as the one used to evolve the flow

Transfers: visual definition

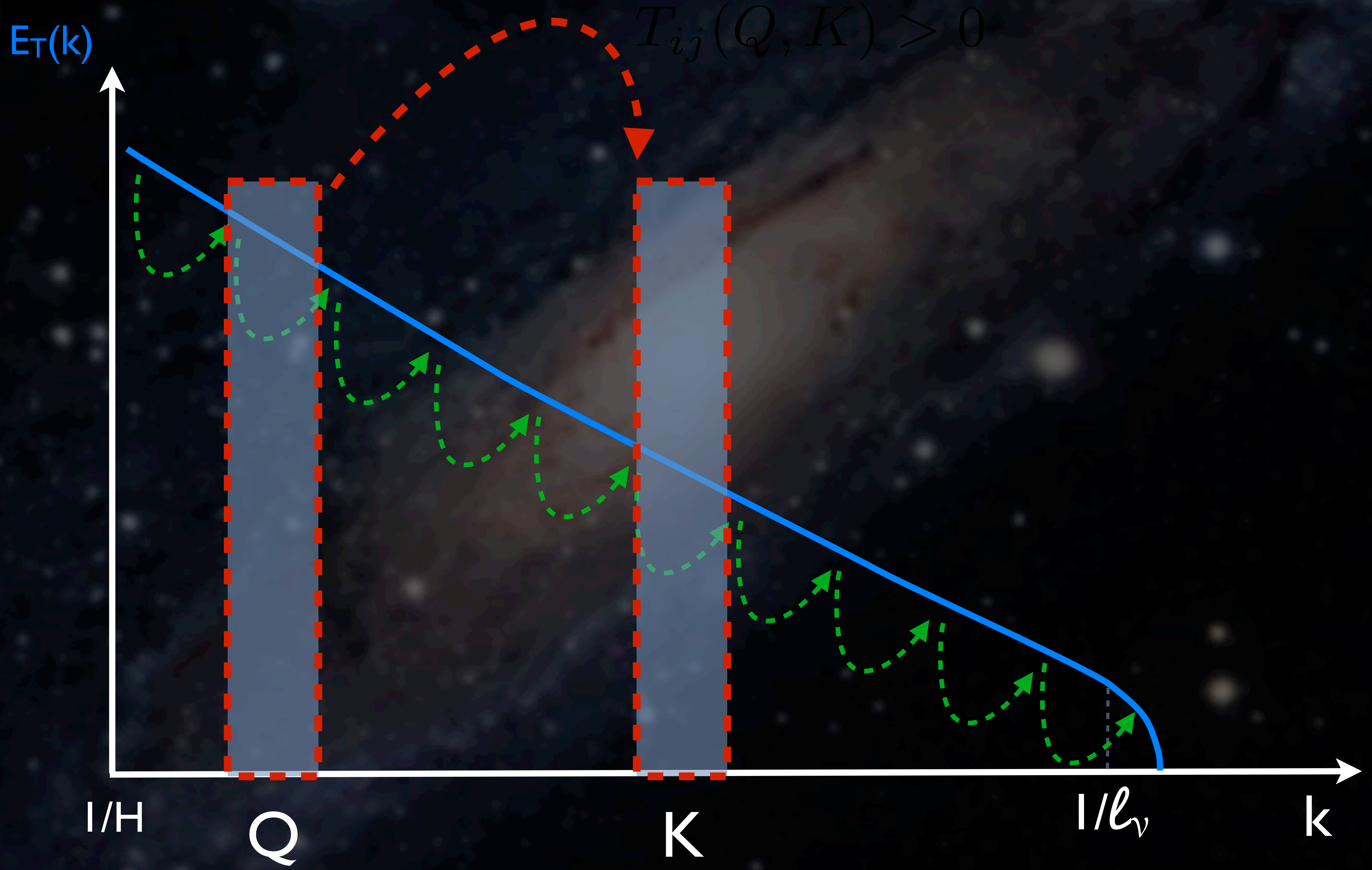

Turbulent energy fluxes

Energy fluxes in spectral space:

$$\mathcal{F}_v(K_0,t) = \sum_{K=K_0}^{K_{\max}} \sum_Q T_{vv}(Q,K) \qquad (1)$$

$$\mathcal{F}_b(K_0,t) = \sum_{K=K_0}^{K_{\max}} \sum_Q T_{bb}(Q,K) \qquad (2)$$

$$\mathcal{F}_x(K_0,t) = \sum_{K=K_0}^{K_{\max}} \sum_Q T_{vb}(Q,K) + T_{bv}(Q,K)$$

Energy fluxes driven by the mean shear (specific to shearing waves)

$$\mathcal{F}_{s,v}(K,t) = \sum_{k'} \frac{q\Omega k_y k_x(t)}{|k(t)|} \frac{\boldsymbol{v}^*_{\boldsymbol{k'}} \cdot \boldsymbol{v}_{\boldsymbol{k'}}}{2} \delta\big(|k(t)| - K\big)$$

$$\mathcal{F}_{s,b}(K,t) = \sum_{k'} \frac{q\Omega k_y k_x(t)}{|k(t)|} \frac{\boldsymbol{B}^*_{\boldsymbol{k'}} \cdot \boldsymbol{B}_{\boldsymbol{k'}}}{2} \delta\big(|k(t)| - K\big)$$

with: $\boldsymbol{k}(t) = \boldsymbol{k'} + q\Omega k'_y t \boldsymbol{e_x}$

Shear flux interpretation

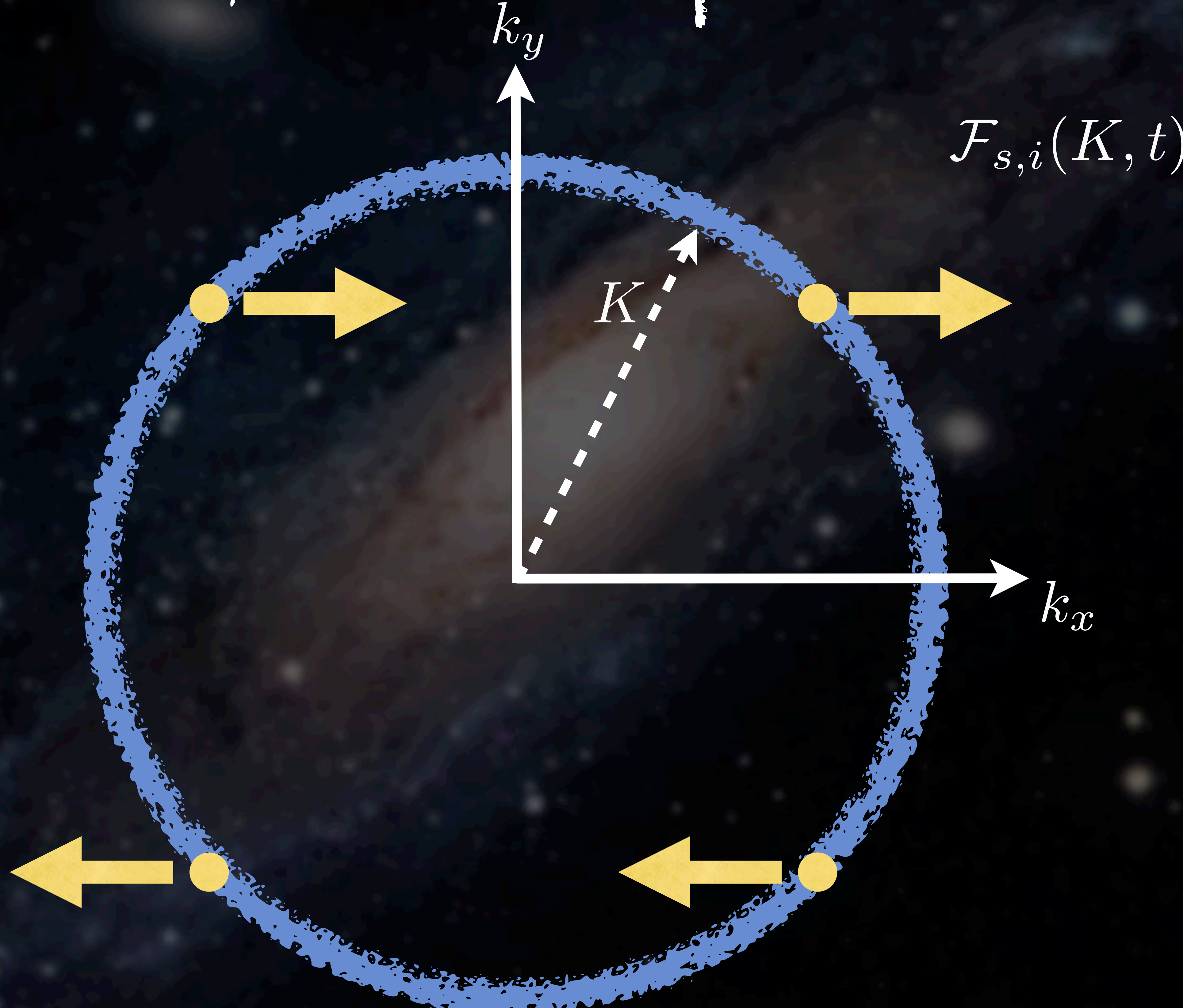

Nonlinear transfer: Fluxes

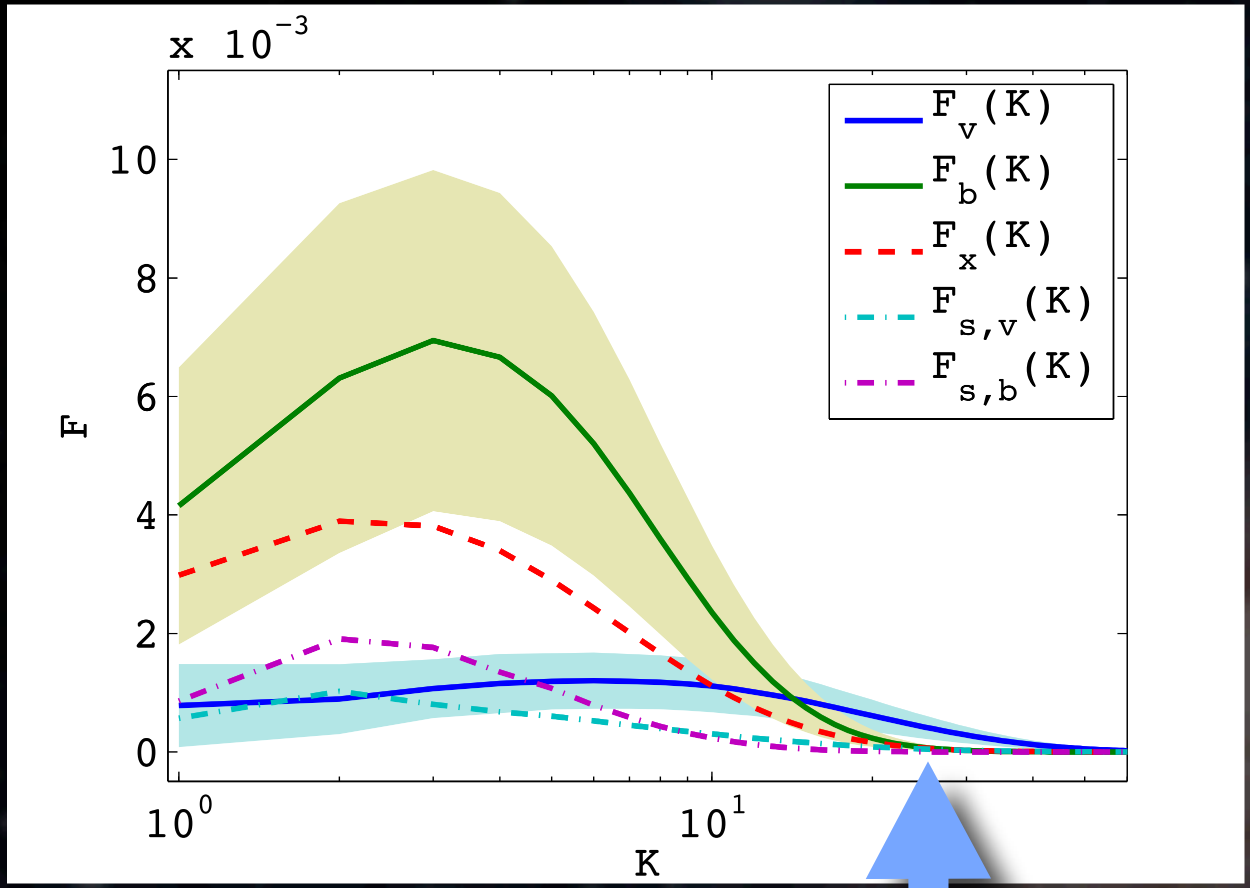

Mean z field, Pm=1/16

pure hydro cascade

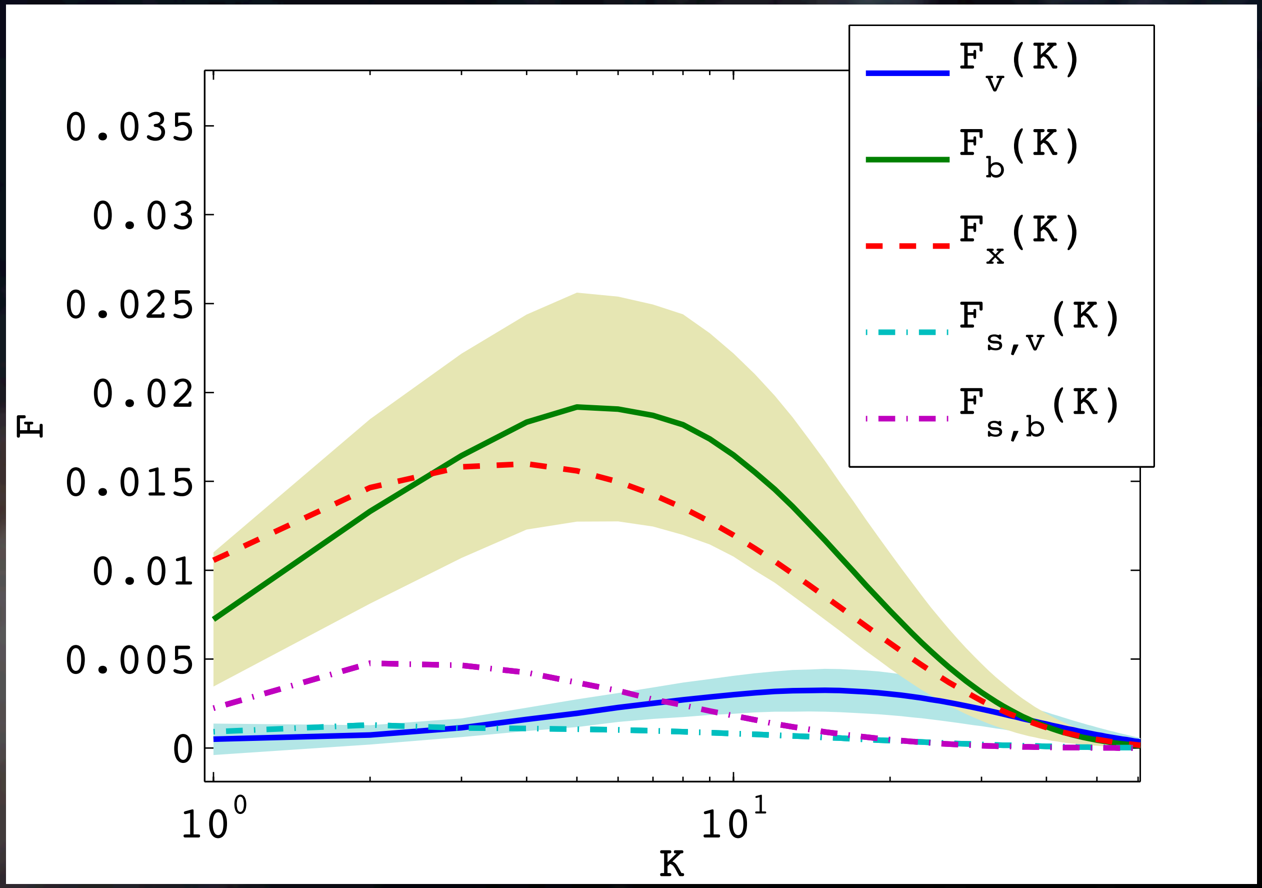

Mean z field, Pm=1/4

- No inertial range
- Dominated by Magnetic energy flux

Nonlinear transfers: locality

Transfer function T_{uu} and T_{bb}: K=1; 5; 20

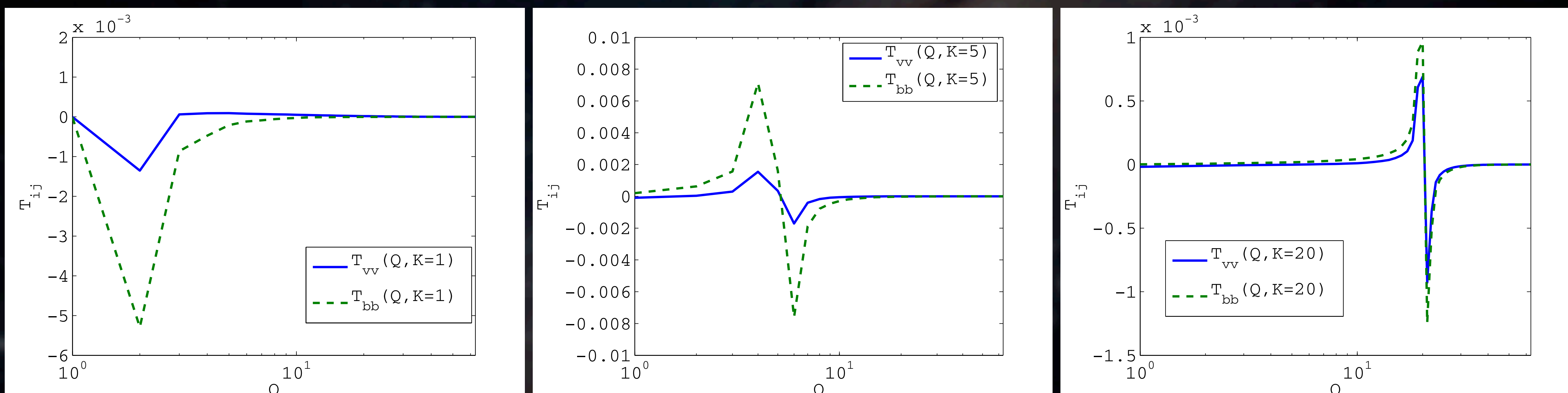

Fig. 7. Transfers function $T_{uu}(Q, K)$ and $T_{bb}(Q, K)$ in the $Pm = 0.25$ run for $K = 1; 5; 20$. These transfers are *local* in Fourier space (see text).

- T_{uu} and T_{bb} are local.

Nonlinear transfers: locality

Transfer function T_{ub} and T_{bu}: K=1; 5; 20

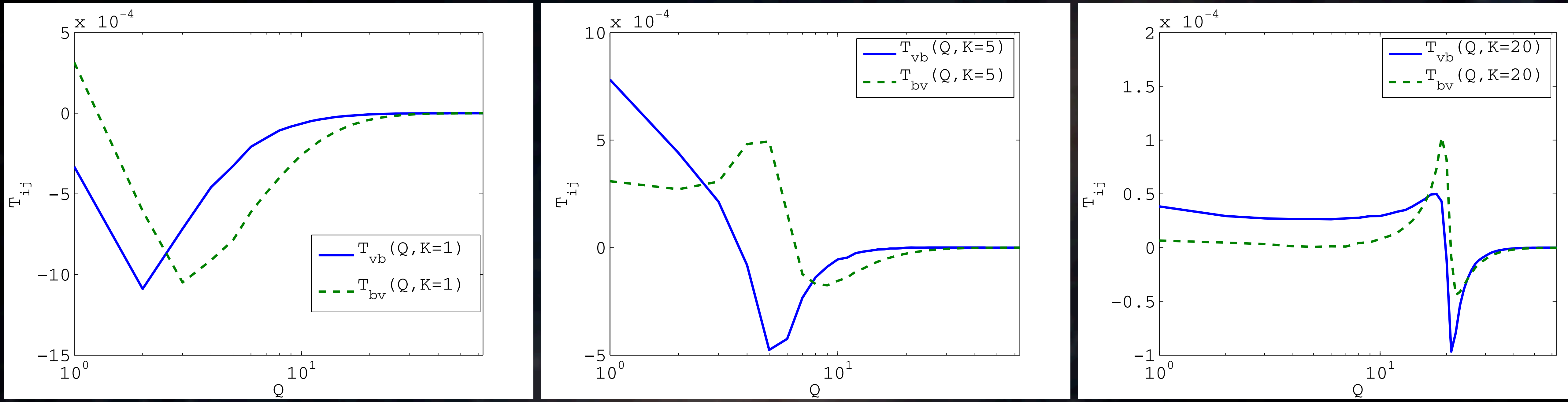

- T_{ub} and T_{bb} have large «wings»: non locality (see also Alexakis *et al.* 2007).
- Direct communication from the largest scales to the dissipation scales.

➡ Non locality is a plausible explanation to the Pm-α effect observed.

The MRI turbulent cascade

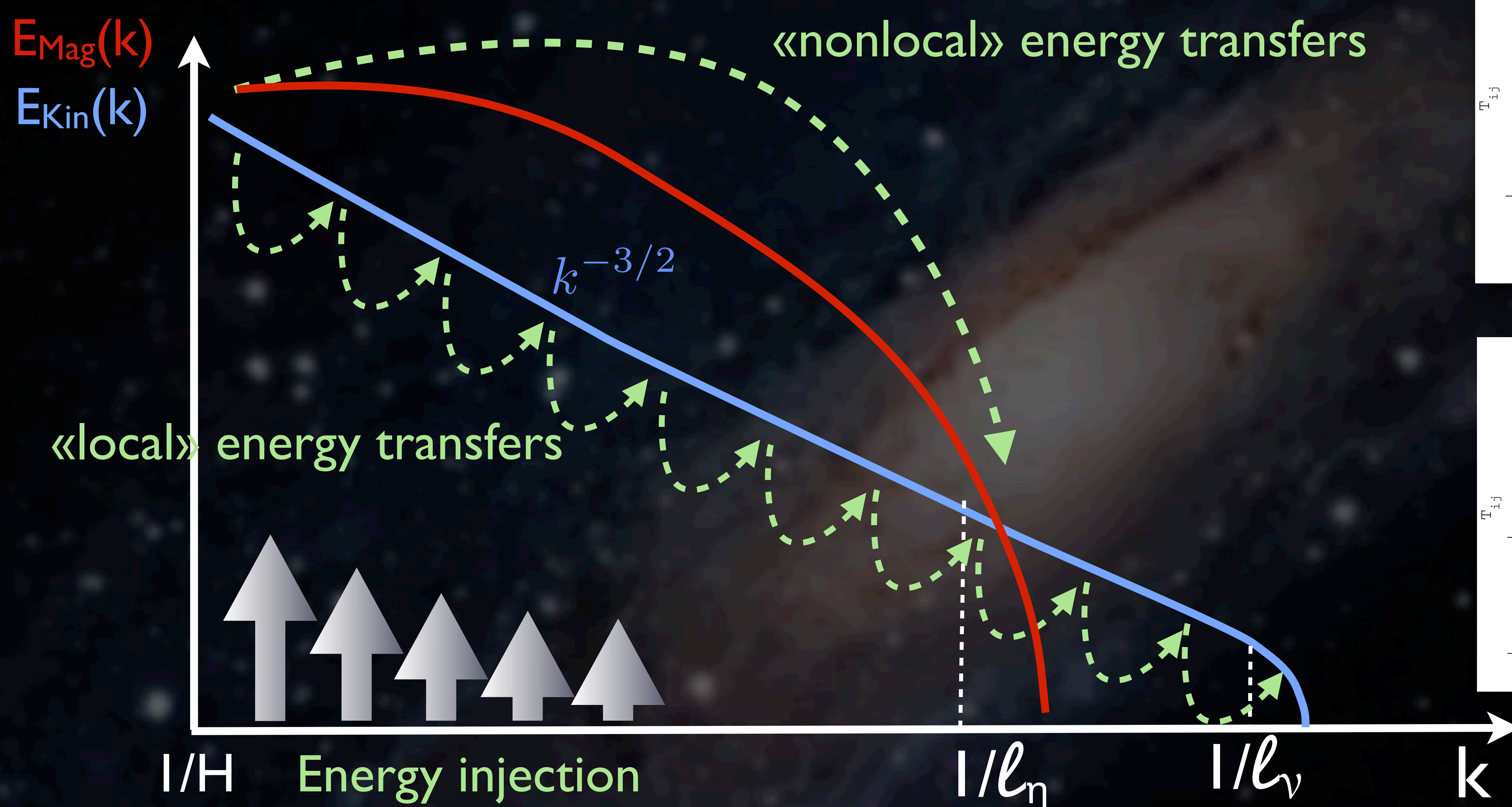

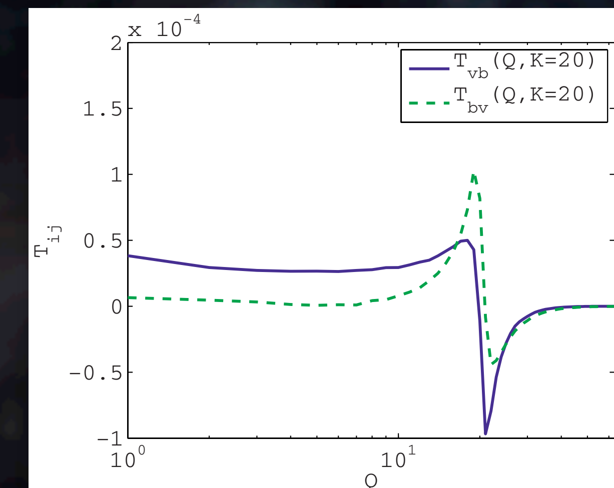

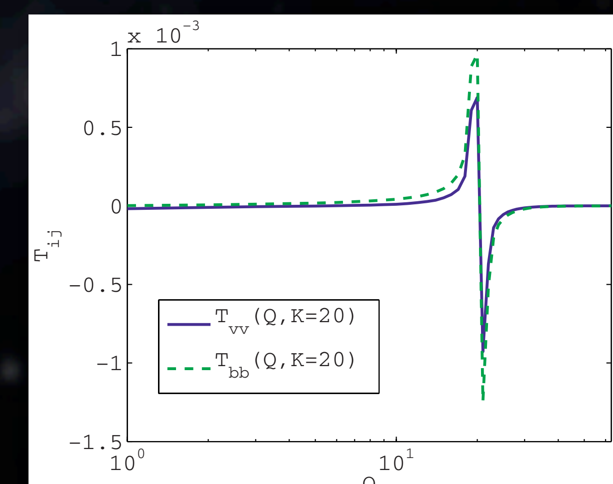

- nonlocal transfers observed in MRI turbulence
- Energy injection on a broad range of scale

→ The global behaviour of MRI (and MHD) turbulence depends on small scale physics!

A Limitation to nonlocal trans

dv_p(l)=<|v(x+l)-v(x)|^p>

Structure function index:
dv_p(l) \propto l^xi_p

where xi_p is the function

- One can show (Aluie & Eyink 2010) that non local transfers are bounded:

$$|T_{ub}(Q,K)| < (\mathrm{const.})Q^{1-\zeta_3^u/3}K^{-2\zeta_3^b/3}$$

Structure function indices

- Which gives for Goldreich-Sridhar phenomenology:

$$|T_{ub}(Q,K)| \sim \varepsilon (K/Q)^{-2/3}$$

- If the scale separation is wide enough, one looses direct energy transfers between transport and dissipation scales

One should loose the Pm-alpha correlation at large enough Rm.
However, this requires ~10,000^3 grid points.

Conclusions

- MRI driven turbulence is highly sensitive to small scale processes
- Strong anisotropy at all scales due to the shear
- Energy injection happens on a wide range of scales
- Helicities (magnetic & cross) don't seem to be important
- Non-local energy transfers are clearly identified between the box scale and the dissipation scales

→ **Current numerical results are biased by the absence of a proper scale separation**

Thank you for your attention